1. Title page:

Complex controls on nitrous oxide flux across a long elevation gradient in the tropical Peruvian Andes

Torsten Diem[1,2], Nicholas J. Morley[1], Adan Julian Ccahuana[3], Lidia Priscila Huaraca Quispe[3], Elizabeth M. Baggs[4], Patrick Meir[5, 6], Mark I.A. Richards[1], Pete Smith[1], and Yit Arn Teh[1,2]*

[1] School of Biological Sciences, University of Aberdeen, UK

[2] Formerly at the School of Geography and Geosciences, University of St Andrews, UK

[3] Universidad Nacional de San Antonio Abad del Cusco, Peru

[4] The Royal (Dick) School of Veterinary Studies, University of Edinburgh

[5] School of GeoSciences, University of Edinburgh, UK

[6] Research School of Biology, Australian National University, Canberra, Australia

[*] Corresponding author; yateh@abdn.ac.uk

2. Abstract

Current bottom-up process models suggest that montane tropical ecosystems are weak atmospheric sources of N_2O, although recent empirical studies from the southern Peruvian Andes have challenged this idea. Here we report N_2O flux from combined field and laboratory experiments that investigated the process-based controls on N_2O flux from montane ecosystems across a long elevation gradient (600-3700 m a.s.l.) in the southern Peruvian Andes. Nitrous oxide flux and environmental variables were quantified in four major habitats (premontane forest, lower montane forest, upper montane forest and montane grassland) at monthly intervals over a 30-month period from January 2011 to June 2013. The role of soil moisture content in regulating N_2O flux was investigated through a manipulative, laboratory-based ^{15}N-tracer experiment. The role of substrate availability (labile organic matter, NO_3^-) in regulating N_2O flux was examined through a field-based litter-fall manipulation experiment and a laboratory-based $^{15}N\text{-}NO_3^-$ addition study, respectively. Ecosystems in this region were net atmospheric sources of N_2O, with an unweighted mean flux of 0.27 ± 0.07 mg $N\text{-}N_2O$ m^{-2} d^{-1}. Weighted extrapolations, which accounted for differences in land surface area among habitats and variations in flux between seasons, predicted a mean annual flux of 1.27 ± 0.33 kg $N_2O\text{-}N$ ha^{-1} $year^{-1}$. Nitrous oxide flux was greatest from premontane forest, which emitted 0.75 ± 0.18 mg $N\text{-}N_2O$ m^{-2} d^{-1}. In contrast, N_2O flux was significantly lower in other habitats, with lower montane forest emitting 0.46 ± 0.24 mg $N\text{-}N_2O$ m^{-2} d^{-1}, montane grasslands emitting 0.07 ± 0.08 mg $N\text{-}N_2O$ m^{-2} d^{-1}, and upper montane forest emitting 0.04 ± 0.07 mg $N\text{-}N_2O$ m^{-2} d^{-1}. Nitrous oxide flux showed weak seasonal variation across the region; only lower montane forest showed significantly higher N_2O flux during the dry season compared to wet season. Manipulation of soil moisture content in the laboratory indicated that N_2O flux was significantly influenced by changes in water-filled pore space (WFPS). The relationship between N_2O flux and WFPS was complex and non-linear, diverging from theoretical predictions of how WFPS relates to N_2O flux. Nitrification made a negligible contribution to N_2O flux, irrespective of soil moisture content, indicating that nitrate reduction was the dominant source of N_2O. Analysis of the pooled data indicated that N_2O flux was greatest at 90 and 50 % WFPS, and lowest at 70 and 30 % WFPS. This trend in N_2O flux suggests a complex relationship between WFPS and nitrate-reducing processes (i.e. denitrification, dissimilatory nitrate reduction to ammonium). Changes in labile organic matter inputs, through the manipulation of leaf litter-fall, did not

alter N_2O flux. Comprehensive analysis of field and laboratory data demonstrated that variations in NO_3^- availability strongly constrained N_2O flux. Habitat – a proxy for NO_3^- availability under field conditions – was the best predictor for N_2O flux, with N-rich habitats (premontane forest, lower montane forest) showing significantly higher N_2O flux than N-poor habitats (upper montane forest, montane grassland). Nitrous oxide flux did not respond to short-term changes in NO_3^- concentration.

3. Introduction

The tropics are the largest source of atmospheric nitrous oxide (N_2O), accounting for at least half of all global N_2O emissions (Hirsch et al., 2006;Huang et al., 2008;Kort et al., 2011;Nevison et al., 2007;Saikawa et al., 2014). The bulk of tropical N_2O emissions come from terrestrial sources, with the largest emissions arising from agricultural land and unmanaged lowland tropical forests (Hirsch et al., 2006;Huang et al., 2008;Kort et al., 2011;Nevison et al., 2007;Saikawa et al., 2014). However, while we have a relatively robust understanding of the global atmospheric budget as a whole (Hirsch et al., 2006;Huang et al., 2008;Saikawa et al., 2014), our knowledge of regional atmospheric budgets, particularly at the sub-continental scale, is much more limited, due to the constraints imposed by the spatial distribution of existing atmospheric sampling networks and ground-based, ecosystem-scale sampling efforts (Kort et al., 2011;Nevison et al., 2004;Nevison et al., 2007;Saikawa et al., 2014).

In order to predict and model N_2O flux at these smaller (sub-continental) spatial scales, bottom-up emissions inventories or process-based models are often used, with emissions estimates constrained by empirical measurements (Werner et al., 2007;Li et al., 2000;Potter et al., 1996;Saikawa et al., 2013). However, these models are only as reliable as the data used to parameterize them; as a consequence, ecosystems that are under-represented in the empirical literature or which are poorly understood may be modelled less accurately, with knock-on effects for larger-scale emissions estimates (Saikawa et al., 2013;Teh et al., 2014;Werner et al., 2007). Nitrous oxide dynamics in montane tropical ecosystems are particularly poorly understood, because past research has concentrated on N_2O flux from lowland *tierra firme* forests (Saikawa et al., 2013;Teh et al., 2014;Werner et al., 2007).

Montane ecosystems, however, are important components of many tropical landscapes, and account for a sizeable land area. For example, in continental South America, montane ecosystems (>500 m a.s.l.) cover more than 8 % of the land surface (Eva et al., 2004), and play key roles in regional carbon (C), nitrogen (N), and greenhouse gas (GHG) dynamics (Girardin et al., 2010;Moser et al., 2011;Teh et al., 2014;Wolf et al., 2012;Wolf et al., 2011). Process-based models predict that N_2O flux from these montane environments are lower than those from the lowland tropics (i.e. <1.0 kg N_2O-N ha^{-1} yr^{-1}) (Saikawa et al., 2013;Werner et al., 2007). However, these models have rarely been tested against empirical data, and several field studies indicate that N_2O flux from montane ecosystems can exceed these prior models' estimates (Corre et al., 2010;Teh et al., 2014;Veldkamp et al., 2008). In some instances, N_2O flux from montane ecosystems can in fact approach emissions from lowland forests, begging the question as to whether or not existing models do, in fact, accurately represent flux from these high elevation ecosystems (Corre et al., 2010;Teh et al., 2014;Veldkamp et al., 2008).

In order to improve our wider understanding of the dynamics and biogeochemistry of N_2O in montane tropical forests, we conducted a combined field and laboratory study to investigate the environmental controls on denitrification and N_2O flux across a long elevation gradient (600-3700 m a.s.l.) in the tropical Peruvian Andes. Prior work from this region indicated that montane ecosystems in this area were stronger sources of N_2O than predicted by bottom-up process models (Teh et al., 2014). In particular, lower elevation premontane and lower montane forests, which account for the majority of the land area in this region (~54 %), showed emission rates that are on par with lowland tropical forests, suggesting that these ecosystems could be important contributors to regional atmospheric budgets (Teh et al., 2014). Nitrous oxide flux appeared to be derived from nitrate reduction (i.e. denitrification, dissimilatory nitrate reduction to ammonium), and was linked to seasonal variations in climate, with N_2O emissions increasing during the dry season compared to the wet season (Teh et al., 2014). However, contrary to theoretical expectations (Davidson, 1991;Firestone and Davidson, 1989;Groffman et al., 2009;Davidson and Verchot, 2000), N_2O flux was not directly correlated with soil moisture content in our field dataset (Teh et al., 2014), raising unresolved questions about the role of seasonal variations in soil moisture content in driving N_2O flux. We hypothesized that the weak relationship between N_2O flux and soil moisture

content was because soil water-filled pore space (WFPS) – an index of soil moisture and a proxy for soil anaerobiosis – normally fell above the theoretical threshold where N_2O flux was constrained by the availability of anaerobic microsites (i.e. ~60 % WFPS) (Davidson, 1991;Firestone and Davidson, 1989;Groffman et al., 2009;Davidson and Verchot, 2000;Teh et al., 2014). Even during the dry season, WFPS rarely fell below this threshold value (Teh et al., 2014), allowing other driving variables, such as nitrate (NO_3^-), to play a more dominant role in regulating N_2O flux (Teh et al., 2014).

In the work presented here, we extended our time series to multi-annual time scales, in order to better understand the role of longer-term climatic variability in modulating N_2O flux. We also conducted a series of manipulative field and laboratory experiments to investigate the mechanistic controls on N_2O flux in greater detail, and to test hypotheses raised by our earlier work (as described below) (Teh et al., 2014). Furthermore, these manipulative experiments were crucial in helping us interpret our time series of field observations, because prior research indicated that the relationship between individual control variables (e.g. WFPS *or* NO_3^-) and N_2O flux were confounded by the simultaneous action of multiple control variables (Teh et al., 2014). The overarching goals of this research were to: investigate how climate and environmental variables regulate N_2O flux over multi-annual time scales; clarify the role of soil moisture as a proximate or distal control on N_2O flux; and evaluate the role of key substrates for nitrate reduction (i.e. labile organic matter, NO_3^-) in driving N_2O flux. Specifically, we hypothesized that:

- **H1.** Enhanced N_2O flux during the dry season (i.e. during periods of reduced soil moisture) is due to an increase in N_2O flux from nitrification and reduced N_2O reduction during denitrification
- **H2.** N_2O flux is poorly correlated with soil water-filled pore space *in situ* because soil moisture content does not normally constrain denitrification under field conditions; however, N_2O flux is closely correlated with water-filled pore space when soil moisture content is more limiting for denitrification (i.e. <60 % WFPS)
- **H3.** N_2O flux increases proportionately with the availability of substrates for denitrification (i.e. NO_3^-, labile organic matter)

In order to address these three objectives and their attendant hypotheses, we quantified N_2O flux and environmental variables from four major habitat types (premontane forest,

lower montane forest, upper montane forest and montane grassland) at monthly intervals over a 30-month period. We also conducted manipulative laboratory experiments that investigated how variations in soil moisture content (WFPS) and NO_3^- availability influenced N_2O flux. In addition, we manipulated labile organic matter availability through a field-based litterfall manipulation study, recognizing that labile organic matter plays an important role in supplying not only the reducing equivalents for nitrate reduction, but also indirectly providing inorganic N for ammonia oxidation and nitrate reduction via N mineralization (Morley and Baggs, 2010;Blackmer and Bremner, 1978;Davidson, 1991;Firestone et al., 1980;Weier et al., 1993).

4. Materials and methods

4.1 Study site

Measurements were conducted on the eastern slope of the Andes in the Kosñipata Valley, Manu National Park, Peru (Figure 1) (Malhi et al., 2010). This 3.02 x 10^6 ha (30,200 km^2) region has been the subject of intensive ecological, biogeochemical and climatological studies since 2003 by the Andes Biodiversity and Ecosystem Research Group (or, ABERG; http://www.andesconservation.org), and contains a series of long-term permanent plots across a 200-3700 m above sea level (m a.s.l) elevation gradient that stretches from the western Amazon to the Andes (Malhi et al., 2010). This part of the Andes experiences pronounced seasonality in rainfall but not in air temperature; the dry season extends from May to September and the wet season from October to April (Girardin et al., 2010). Thirteen sampling plots (approximately 20 x 20 m each) were established at four different habitats across a gradient spanning 600-3700 m a.s.l., including premontane forest (600 – 1200 m a.s.l.; n = 3 plots), lower montane forest (1200 – 2200 m a.s.l.; n = 3 plots), upper montane forest (2200 – 3200 m a.s.l.; n = 3 plots), and montane grasslands (3200 – 3700 m a.s.l.; n = 4 plots; colloquially referred to as “puna”) (Figure 1). In premontane forest, sampling plots were established in Hacienda Villa Carmen, a 3,065 ha biological reserve operated by the Amazon Conservation Association (ACA), containing a mixture of old-growth forest, secondary forest and agricultural plots (Teh et al., 2014). Sampling for soil gas flux was concentrated in the old-growth portions of the reserve. For lower montane and upper montane forests, sampling plots were established adjacent to or within existing 1 ha

177 permanent sampling plots established by ABERG (Teh et al., 2014). Sampling plots were also
178 established in montane grasslands (Teh et al., 2014). To capture a representative range of
179 environmental conditions, mesotope-scale (100 m-1 km scale landforms) topographic
180 features were sampled (Belyea and Baird, 2006). Mesotopic features include ridges, slopes,
181 flats and a high elevation basin. The latter two landforms include wet, grassy lawns with no
182 discernible grade, and a peat-filled depression, respectively. Summary site descriptions are
183 provided in Table 1. Data on soil properties were collected as part of this study, while mean
184 annual precipitation is from earlier research by ABERG (Girardin et al., 2010).
185
186 **4.2 Soil-atmosphere exchange**
187 Field sampling was performed over a 30-month period from January 2011 to June 2013 for
188 all habitats except for premontane forest. Due to circumstances outside our control, only 24-
189 months of data were collected for premontane forest, with sampling commencing in July
190 2011. Soil-atmosphere flux was collected monthly, except where flooding or landslides
191 prevented safe access by investigators to the study sites. Gas exchange rates were
192 determined with five replicate gas flux chambers deployed in each of the thirteen plots (n =
193 65 flux observations per month). All representative landforms were sampled in each habitat
194 (Table 1).
195
196 Soil-atmosphere flux of CH_4, N_2O and CO_2 were determined using a static flux chamber
197 approach (Livingston and Hutchinson, 1995), although only N_2O flux is reported here.
198 Methane and CO_2 flux are discussed in detail in another publication (Jones et al., 2016).
199 Static flux chamber measurements were made by enclosing a 0.03 m^2 area with cylindrical,
200 opaque (i.e. dark), two-component (i.e. base and lid) vented chambers with a ~8 L volume.
201 Chamber bases were permanently installed to a depth of approximately 5 cm and inserted
202 >1 month prior to the commencement of sampling, in order to minimize potential artefacts
203 from root mortality following base emplacement (Varner et al., 2003). Chamber lids were
204 fitted with small computer case fans to promote even mixing in the chamber headspace
205 (Pumpanen et al., 2004). Headspace samples were collected from each flux chamber over a
206 30-minute enclosure period, with samples collected at 4 discrete intervals, 7.5 minutes
207 apart, using a gastight syringe. Gas samples were stored in evacuated Exetainers® (Labco
208 Ltd., Lampeter, UK), shipped to the UK by courier, and subsequently analysed for CH_4, N_2O

and CO_2 concentrations with a Thermo TRACE GC Ultra (Thermo Fisher Scientific Inc., Waltham, Massachusetts, USA) at the University of St Andrews. Chromatographic separation was achieved using a Porapak-Q column, and analyte concentrations quantified using a flame ionization detector (FID) for CH_4, electron capture detector (ECD) for N_2O, and methanizer-FID for CO_2. Instrumental precision was determined by repeated analysis of standards and was better than 5 % for all detectors. Gas flux rates were determined using the R HMR package to plot best-fit lines to the data for headspace concentration against time for individual flux chambers (Pedersen et al., 2010;Team, 2012). Gas mixing ratios (ppm) were converted to areal flux by using the Ideal Gas Law to solve for the quantity of gas in the headspace (on a mole or mass basis), normalized by the surface area of each static flux chamber (Livingston and Hutchinson, 1995). Measurements resulting in zero net flux were included in our dataset.

4.3 Environmental variables

To investigate the effects of environmental variables on trace gas dynamics, we determined soil moisture, soil oxygen content in the 0-10 cm depth, soil temperature, and air temperature at the time of flux sampling. Volumetric soil moisture content was determined using portable soil moisture probes (ML2x ThetaProbe, Delta-T Device Ltd., Cambridge, UK) inserted into the substrate immediately adjacent to each flux chamber (<5 cm from each chamber base; depth of 0-10 cm). Soil moisture content is reported here as water-filled pore space (WFPS), and is calculated using the measurements of volumetric water content and bulk density (Breuer et al., 2000). Soil O_2 concentration was determined using the approach described by Teh et al. (2014). Soil temperature (0-10 cm depth), chamber temperature and air temperature was determined using type K thermocouples (Omega Engineering Ltd., Manchester, UK). Data on aboveground litter-fall, meteorological variables (i.e. photosynthetically active radiation, air temperature, relative humidity, rainfall, wind speed, wind direction), continuous plot-level soil moisture (10 and 30 cm depths) and soil temperature (0, 10, 20 and 30 cm depths) measurements were also collected, but are not reported in this publication.

Resin-extractable inorganic N flux (i.e. ammonium, NH_4^+; nitrate, NO_3^-) were quantified in all plots using a resin bag approach (Templer et al., 2005;Subler et al., 1995). From August 2011

onwards, ion exchange resin bags (n = 15 resin bags per elevation) were deployed at the bottom of the plant rooting zone (i.e. 0-10 cm depth in premontane forest, lower montane forest and montane grasslands; 0-15 cm in upper montane forest), following established protocols (Templer et al., 2005;Subler et al., 1995). Samples were collected at monthly intervals (where possible) for determination of monthly, time-averaged NH_4^+ and NO_3^- flux (Subler et al., 1995). For some plots, this sampling frequency was periodically disrupted due to natural hazards (i.e. landslides, river flooding) preventing safe access to the study sites. Resin bags were shipped to the University of Aberdeen after collection from the field, inorganic N was extracted using 2 M KCl and concentrations determined colourimetrically using a Burkard SFA2 continuous-flow analyser (Burkard Scientific Ltd., Uxbridge, UK) (Templer et al., 2005;Subler et al., 1995).

4.4 Water-filled pore space manipulation study

We investigated the effects of WFPS on N_2O flux derived from nitrate reduction or nitrification rates using a ^{15}N tracer experiment. Soil cores for all habitats were collected from the 0-10 cm depth, and were not fully air-dried nor sieved prior to incubation. Soils were distributed into glass jars and adjusted to 10% below the target WFPS values of 30%, 50%, 70% and 90%, either by letting the soils partially air-dry or by adding water to them, depending on the WFPS of the soils at the time of collection (n = 5 for each ^{15}N addition and 3 controls for each WFPS for a total of n = 212; see Table 2). Additional de-ionized water, containing the ^{15}N tracers, was subsequently added gravimetrically to raise WFPS to target levels. The exception to this was for the upper montane forest, where samples were collected from the 0-10 cm depth of the mineral soil, but not from the organic layer. The reason for this is that the mineral soil layer in the upper montane forest is overlain by a thick organic horizon up to 17 cm deep, consisting of poorly decomposed leaves, roots, and humic materials; very akin to low density peat (Zimmermann et al., 2012;Zimmermann et al., 2009a;Zimmermann et al., 2009b). In contrast, the organic matter in the upper 10 cm soil layer in the other habitats is closely intermixed with the mineral phase, and does not normally constitute a distinct mineral-free horizon. Thus, to sample mineral soil in the upper montane forest, we had to sample beneath this thick organic horizon.

Two different types of ^{15}N-tracers (30 atom %) were applied to the soils in order to determine the proportion of N_2O derived from nitrate reduction and nitrification (Bateman and Baggs, 2005). $^{14}N\text{-}NH_4{}^{15}N\text{-}NO_3$ was used to quantify the amount of N_2O produced by nitrate reduction, while $^{15}N\text{-}NH_4{}^{15}N\text{-}NO_3$ was used to quantify the amount of N_2O produced from both nitrate reduction and nitrification. The difference between the two was used to calculate the amount of N_2O derived from nitrification alone. After application of the tracers, the jars were sealed, and gas samples taken at 0, 6, 12, 24, 36 and 48 hours to determine rates of gas flux. Nitrous oxide yield was calculated as the ratio of $^{15}N\text{-}N_2O$ flux : $^{15}N\text{-}N_2O$ flux + $^{15}N\text{-}N_2$ flux. Soils were sampled at the end of the experiment for NO_3^- concentration, NH_4^+concentraion, and total C and N content.

Soil gas concentrations (N_2O, CO_2 and CH_4) were measured on a GC as described in section 4.2, while $^{15}N\text{-}N_2$ and $^{15}N\text{-}N_2O$ were measured on a SerCon 20:20 isotope ratio mass spectrometer equipped with an ANCA TGII pre-concentration module (SerCon Ltd., UK). The coefficient of variation (CV; an index of instrumental precision) for repeated analysis of gas concentration and isotope standards was <5 %. $^{15}N\text{-}N_2O$ and $^{15}N\text{-}N_2$ fluxes were calculated from the ^{15}N atom percent excess of the samples compared to the controls using the HMR package (Pedersen et al., 2010).

4.5 Litter-fall manipulation experiments

We conducted a field-based litter-fall manipulation experiment to test for the effects of variations in labile organic matter availability on trace gas flux. This study took place over a 14-month period (April 2012 to June 2013), and consisted of 4 experimental treatments (control, +50 % litter addition, +100 % litter addition, litter removal) implemented across 3 habitats (premontane forest, lower montane forest, upper montane forest), with 6 replicate plots per treatment per habitat (each treatment plot was 0.5 x 0.5 m in size; n = 24 observations per habitat; n = 72 observations per sampling increment). Leaf litter addition rates for the +50 % and +100 % litter addition treatments were determined based on prior research from this study site, and fell within the natural range of variability observed across this elevational gradient (Girardin et al., 2010).

Litter-fall for the litter addition treatments was collected monthly in litter baskets (n = 3 litter baskets per treatment plot for a total of n = 18 per habitat). These data were also used to determine the background rates of leaf litter-fall among habitats. For the control, litter inputs simply reflected natural background litter-fall rates. For the +50 % and +100 % litter addition treatments, background litter inputs were supplemented with additional litter taken from the litter baskets. Briefly, wet litter was weighed in the field using portable scale, gently mixed (homogenized), and then re-distributed to the +50 % and +100 % litter addition plots in amounts proportional to the average amount of wet litter that fell into the litter baskets over the course of the month. As a consequence, the amount of litter added in the two litter addition treatments was not fixed but varied according to the natural background rate of litter-fall. For the litter removal treatment, leaf litter was removed from the forest floor at the start of the experiment, and 3mm nylon mesh was placed over the surface of the treatment plot to prevent further litter ingress to the soil surface. Any debris accumulating on the mesh was removed at monthly intervals.

Trace gas flux and environmental variables were determined at 7 time points over the course of the 14-month experiment using the methods described in section 4.2. In addition, soil moisture (WFPS from the 0-10 cm depth), soil temperature (0-10 cm depth), air temperature, soil gas concentrations (O_2, CH_4, N_2O, CO_2) from the 0-10 cm and 20-30 cm depths, litter C, and litter N were determined concomitantly. Litter C and N content was determined on a Carlo-Erba NA 2500 elemental analyser (CE Instruments Ltd, Wigan, UK) at the University of Aberdeen.

4.6 Nitrate addition experiment

To quantify the effect of NO_3^- availability on N_2O flux, we conducted a $^{15}N\text{-}NO_3^-$ addition experiment. Background concentrations of NO_3^- were determined prior to the start of experiment using soil subsamples (n = 5 per elevation), after which the soils from each habitat were divided into three treatment groups, and supplemented with surplus NO_3^- which raised these background levels by +50 %, +100 %, and +150 % (Table 2). The NO_3^- added to the soil in each of the treatments was enriched with ^{15}N in order to trace the conversion of nitrate to gaseous N products ($^{15}N\text{-}N_2O$, $^{15}N\text{-}N_2$) (Baggs, 2003;Bateman and Baggs, 2005).

Soil cores were sampled from 0-10 cm for each habitat (n = 6 soil cores per habitat), with the exception for upper montane forest, where two separate sets of cores were collected, one from the organic layer (O horizon; n = 6) and the other from the mineral layer (A horizon; n = 6). Soil samples were then shipped to the University of Aberdeen and sampled within one week of arrival. Transport times from Peru to the UK varied between one and two weeks. Five of these soil cores, one for each replicate, were split into four equal parts (3 treatment samples and one control sample) and distributed into 1 L screw top jars (Kilner, UK). A small soil subsample from each core was used to determine WFPS, background NO_3^- content (extracted in 100ml 1M KCl for a 10g soil sample prior to the start of the experiment), as well as total C and N content. If necessary, the samples were gravimetrically amended with water until the cores reached 80% WFPS. Soil cores were kept under constant conditions for 3 days before the start of the experiment to minimize the effects of changing water content on soil processes.

At the start of the experiment, dissolved ^{15}N-labelled KNO_3 (30 atom %) was added according to the measured NO_3^- concentrations of each core to reach the required NO_3^- concentration for each treatment (Table 2). Initial NO_3^- concentration (prior to ^{15}N addition) averaged (± standard error) 157 ± 12 µg N g $soil^{-1}$ for pre-montane forest, 140 ± 12 µg N g $soil^{-1}$ for lower montane forest, 19 ± 7 µg N g $soil^{-1}$ for upper montane forest organic layer soil, 18 ± 5 µg N g $soil^{-1}$ for upper montane forest mineral layer soil, and 6 ± 2 µg N g $soil^{-1}$ for montane grassland soil (Table 2). The jars were then sealed with lids fitted with a two-way stopcock to allow for gas sampling. Gas samples were taken with gas tight syringes, and stored in pre-evacuated containers for determination of ^{15}N-N_2, ^{15}N-N_2O, N_2O, CO_2 and CH_4 content. Isotope samples (150 ml) were stored in 100 mL serum bottles and gas concentration samples (20 ml) were stored in 12 ml Exetainers® (Labco Ltd., Lampeter, UK). After gas sampling, the stopcock was opened to allow the sampled air from the jar to be replaced by lab air, and lab air was sampled to allow for correction of the gas concentrations in the jars due to dilution. Samples were taken at 0, 6, 12, 24, 36, and 48 hours, after which the jars were opened and soil was sampled for determination of NO_3^-, NH_4^+ and total C and N. Gas flux, isotopic and elemental concentrations were determined according to the methods described previously.

4.7 Statistics

Statistical analyses were performed using JMP IN Version 8 (SAS Institute, Inc., Cary, North Carolina, USA) or R (Team, 2012). Residuals were checked for heteroscedasticity and homogeneity of variances. Where necessary, the data were transformed using a Box-Cox procedure to meet the assumptions of analysis of variance. Analysis of variance (ANOVA) or Generalized Linear Models were used to evaluate the effect of categorical variables (i.e. site, season, topography) on trace gas flux and environmental variables. Analysis of covariance (ANCOVA) was performed on Box-Cox transformed data to investigate the combined effects of categorical variables and environmental factors (e.g. water-filled pore space, soil oxygen content, air temperature, soil temperature, etc.) on trace gas flux. Non-parametric tests were employed where Box-Cox transformation was unable to normalize the data, homogenize the variances, or where the residuals still showed strong trends even after Box-Cox transformation. Means comparisons were performed using Fisher's Least Significant Difference test (Fisher's LSD). Statistical significance was determined at the $P < 0.05$ level, unless otherwise noted. Values are reported as means and standard errors (± 1 SE). Statistical analyses for the field data were conducted on plot-averaged data to avoid pseudo-replication.

5. Results

5.1 Variations in N_2O flux among habitats and between seasons

The overall mean N_2O flux for the entire dataset was 0.27 ± 0.07 mg N-N_2O m^{-2} d^{-1}, with a range from -8.40 to 75.0 mg N-N_2O m^{-2} d^{-1}. We investigated the effect of habitat, season, topography, and the interaction of habitat by season on N_2O flux by using a three-way ANOVA on plot-averaged data ($F_{10,307}$ = 3.28, $P < 0.0005$; Supplementary Online Materials Table S1A). We found that there was a significant effect of habitat ($P < 0.003$) and an effect of season at the borderline of statistical significance ($P < 0.07$). However, we found no effect of topography and no habitat by season interaction effect on N_2O flux. Habitat accounted for the largest proportion of variance in the dataset (4.3 %), while season accounted for only 1.0 % of the variance (Supplementary Online Materials Table S1A).

Among habitats, the overall trend was towards the highest flux from premontane forest (0.75 ± 0.18 mg N-N_2O m^{-2} d^{-1}), followed by lower montane forest (0.46 ± 0.24 mg N-N_2O m^{-2} d^{-1}), montane grasslands (0.07 ± 0.08 mg N-N_2O m^{-2} d^{-1}), and upper montane forest (0.04 ± 0.07 mg N-N_2O m^{-2} d^{-1}) (Figure 2a). Multiple comparisons tests indicated that only premontane forests showed statistically higher flux than the others (Fisher's LSD, $P < 0.05$); while there were numerical differences in mean flux among the other habitats, large variances meant that they had overlapping ranges of flux (Figure 2a).

The borderline significant effect of season ($P < 0.07$) reflected an overall trend of higher dry season (0.51 ± 0.18 mg N-N_2O m^{-2} d^{-1}) compared to wet season flux (0.15 ± 0.07 mg N-N_2O m^{-2} d^{-1}) in the pooled dataset (Table 3). However, part of why the effect of season was weak was because only lower montane forest showed significant variability between seasons (Fisher's LSD, $P < 0.05$), while the other three habitats did not show significant seasonal differences in flux (Fisher's LSD, $P < 0.05$).

Even though the effect of topography alone was not statistically significant, N_2O flux from flat sites were significantly higher (0.62 ± 0.28 mg N-N_2O m^{-2} d^{-1}) than from the basin site (-0.18 ± 0.16 mg N-N_2O m^{-2} d^{-1}) (Fisher's LSD, $P < 0.05$). However, there was no significant difference between flat sites and either slope or ridge sites (0.24 ± 0.09 mg N-N_2O m^{-2} d^{-1} and 0.20 ± 0.08 mg N-N_2O m^{-2} d^{-1}, respectively) (Fisher's LSD, $P > 0.05$).

For each habitat, we also compared individual wet and dry seasons against each other using multiple comparisons tests (e.g. dry season 2012 vs wet season 2012; dry season 2012 vs dry season 2013, etc.) to determine if there was significant inter-annual (i.e. year-on-year) variation in N_2O flux among seasons. Consistent with our three-way ANOVA results, we found that only lower montane forest showed significant variation among multiple dry and wet seasons, whereas the other habitats showed no significant trends. For lower montane forest, we observed significantly higher dry season flux in 2011 compared to wet and dry seasons in all other years ($P < 0.05$; Figure 3b).

5.2 Variations in environmental conditions among habitats and between seasons

We investigated the effect of habitat, season, topography, and the interaction of habitat by season on environmental variables using a three-way ANOVA on plot-averaged data. The environmental variables examined here were: water-filled pore space (WFPS) in the 0-10 cm depth, gas-phase soil oxygen content in the 0-10 cm depth, soil temperature, air temperature, and resin-extractable inorganic N flux (NH_4^+, NO_3^-).

Water-filled pore space varied significantly as a function of habitat, season, habitat by season, and topography ($F_{10,304}$ = 637.96, P < 0.0001; Table 3; Figure 2b; Figure 3; Supplementary Online Materials Table S1B). Habitat accounted for the largest proportion of variance in the model (78.1 %), followed by season (0.6 %), habitat by season interaction (0.6 %), and topography (0.4 %) (Supplementary Online Materials Table S1B). Each habitat differed significantly from the others (Fisher's LSD, P <0.05), with the highest WFPS observed in montane grassland (88.4 ± 0.3 %), followed by premontane forest (51.6 ± 1.3 %), lower montane forest (39.0 ± 0.9 %), and upper montane forest (35.0 ± 1.5 %) (Figure 2b). WFPS varied significantly between seasons (t-Test, P < 0.05), with a mean dry season value of 52.1 ± 2.4 % compared to a mean wet season value of 59.5 ± 1.6 % (Table 3). The significant habitat by season interaction is due to the fact that some habitats showed seasonal trends in WFPS whereas others did not. Whereas lower montane and upper montane forests all showed a significant reduction in WFPS during the dry season, premontane forest and montane grasslands showed no seasonal differences in WFPS (Table 3, Figure 3). For topography, the main effect was that the basin landform had significantly higher WFPS than the other landforms. The basin landform showed a mean WFPS of 89.3 ± 0.1 % whereas WFPS in other landforms ranged from 51.7 ± 2.2 to 57.7 ± 2.7 %.

Soil oxygen in the 0-10 cm depth varied significantly as a function of habitat, habitat by season, and topography ($F_{10,242}$ = 27.70, P < 0.0001; Table 3; Supplementary Online Materials Table S1C). Habitat accounted for the largest proportion of variance in the model (66.9 % of the total variance), followed by topography (8.4 %), habitat by season (3.5 %) (Supplementary Online Materials Table S1C). For habitat, multiple comparisons tests indicated that only montane grasslands showed significantly lower soil O_2 content than the other habitats (13.5 ± 0.6 %), while the others showed statistically similar soil O_2 values to each other (18.6 ± 0.2 to 19.5 ± 0.1 %; Fisher's LSD, P < 0.05). For topography, multiple

462 comparisons tests indicated that the basin landform showed statistically lower soil O_2
463 content than the other landforms (7.4 ± 2.3 %), whereas the other topographic features
464 showed statistically similar values, ranging from 16.9 ± 0.6 to 18.2 ± 0.2 % (Fisher's LSD, $P <$
465 0.05). The significant habitat by season interaction was due to the fact that only montane
466 grassland showed a significant difference in O_2 content between wet and dry season,
467 whereas other habitats showed similar soil O_2 values (Table 3).
468
469 For soil temperature, the effects of habitat, season, habitat by season, and topography were
470 all significant ($F_{10,292}$ = 790.7, P < 0.0001; Supplementary Online Materials Table S1D).
471 Habitat accounted for the largest proportion of variance in the model (85.5 % of the total
472 variance), followed by season (1.4%), habitat by season interaction (0.5 %), and topography
473 (0.3 %) (Supplementary Online Materials Table S1D). Each habitat differed significantly from
474 the others (Fisher's LSD, P <0.05), with the highest soil temperature observed for
475 premontane forest (20.5 ± 0.1 °C), followed by lower montane forest (17.8 ± 0.1 °C), upper
476 montane forest (11.5 ± 0.1 °C), and montane grasslands (10.6 ± 0.2 °C). Soil temperature
477 varied significantly between season (t-Test, $P < 0.05$), with a mean dry season value of 13.9 ±
478 0.4 °C compared to a mean wet season value of 15.1 ± 0.3 °C. The significant habitat by
479 season interaction is due to the fact that some habitats showed more pronounced seasonal
480 trends in soil temperature than others, although the overall pattern of cooler dry season
481 compared to wet season soil temperatures holds across all habitats (Table 3). For
482 topography, the flat landforms showed significantly higher soil temperatures than the others
483 (16.0 ± 0.5 °C), the basin landform showed significantly lower values (10.8 ± 0.4 °C), whereas
484 ridge and slope landforms showed similar values to each other (14.3 ± 0.4 °C and 14.7 ± 0.4
485 °C, respectively) (Fisher's LSD, $P < 0.05$).
486
487 For air temperature, only the effect of habitat was significant ($F_{10,292}$ = 103.2, P < 0.0001;
488 Table 3; Supplementary Online Materials Table S1E). A multiple comparisons test indicated
489 that each habitat showed significantly different temperatures compared to the others
490 (Fisher's LSD, $P < 0.05$). Premontane forest showed the highest air temperatures (21.0 ± 0.3
491 °C), followed by lower montane forest (18.7 ± 0.2 °C), upper montane forest (12.7 ± 0.2 °C),
492 and montane grassland (11.7 ± 0.3 °C). Other variables did not significantly affect air
493 temperature.

494

495 For resin-extractable NH_4^+ flux, even though the three-way ANOVA model was not
496 statistically significant, the overall trend was towards significantly lower NH_4^+ flux in the dry
497 season (9.6 ± 0.7 μg N-NH_4 g $resin^{-1}$ d^{-1}) compared to the wet season (22.3 ± 3.6 μg N-NH_4 g
498 $resin^{-1}$ d^{-1}) ($F_{10,164}$ = 1.3, P > 0.2; Table 3; Supplementary Online Materials Table S1F).
499

500 Resin-extractable NO_3^- flux showed different patterns from NH_4^+ flux, with significant effects
501 of habitat, topography, and habitat by season but not of season alone ($F_{10,164}$ = 39.0, P <
502 0.0001; Figure 2c; Table 3; Supplementary Online Materials Table S1G). Habitat accounted
503 for the largest proportion of the variance (61.5 %), followed by topography (4.7 %), and
504 habitat by season (1.9 %). Premontane forest showed the highest NO_3^- flux (22.6 ± 2.0 μg N-
505 NO_3 g $resin^{-1}$ d^{-1}), followed by lower montane forest (10.0 ± 1.2 μg N-NO_3 g $resin^{-1}$ d^{-1})
506 (Fisher's LSD, P < 0.05; Figure 2c). Upper montane forest (1.1 ± 0.2 μg N-NO_3 g $resin^{-1}$ d^{-1}) and
507 montane grassland (1.7 ± 0.3 μg N-NO_3 g $resin^{-1}$ d^{-1}) showed significantly lower NO_3^- flux than
508 the other two habitats (Fisher's LSD, P < 0.05; Figure 2c), with values that were not
509 significantly different from each other (Fisher's LSD, P > 0.05; Figure 2c). For the effect of
510 topography, multiple comparisons tests indicated that flat landforms (12.1 ± 1.8 μg N-NO_3 g
511 $resin^{-1}$ d^{-1}) and slope landforms (10.2 ± 1.6 μg N-NO_3 g $resin^{-1}$ d^{-1}) differed significantly from
512 ridge landforms (6.6 ± 1.4 μg N-NO_3 g $resin^{-1}$ d^{-1}) (Fisher's LSD, P < 0.05). The basin landform
513 (3.8 ± 1.3 μg N-NO_3 g $resin^{-1}$ d^{-1}), despite the lower mean values, showed an overlapping
514 range with the other landforms (Fisher's LSD, P > 0.05). The habitat by season interaction
515 was due to the fact that upper montane forest shows a significant seasonal fluctuation in
516 resin-extractable NO_3^- (Fisher's LSD, P < 0.05), whereas the other habitats show no significant
517 seasonal trend (Fisher's LSD, P > 0.05; Table 3).
518

519 **5.3 Effects of environmental variables on N_2O flux**

520 For the whole dataset, the relationship between N_2O flux and environmental variables was
521 examined using an ANCOVA on Box-Cox transformed data with habitat, season, topography,
522 and environmental variables as covariates. Environmental variables included WFPS, oxygen,
523 air temperature, soil temperature, and resin-extractable inorganic N flux (NH_4^+ and NO_3^-).
524 The ANCOVA model as a whole was not statistically significant (P > 0.4). However, we found
525 that individual factors were weakly but significantly correlated with N_2O flux for the pooled

dataset. These included soil temperature (r^2= 0.04, *P* <0.0004), air temperature (r^2= 0.04, *P* <0.0008), and resin-extractable NO_3^- flux (r^2= 0.03, *P* <0.03). Water-filled pore space also showed a very weak negative correlation with N_2O flux at the borderline of statistical significance (r^2= 0.01, *P* <0.06).

For individual habitats, we explored how variations in environmental conditions influenced N_2O flux using multiple regression, with WFPS, oxygen, soil temperature, air temperature, resin-extractable NH_4^+ flux, and resin-extractable NO_3^- flux as explanatory variables. Only the multiple regression analysis for lower montane forest showed a borderline significant result, though only at the *P* < 0.07 level (r^2 = 0.36). The multiple regression models for all the other habitats were not statistically significant (*P* > 0.4). Lower montane forest was the only habitat that showed a significant effect of season on N_2O flux (section 5.1), and our multiple regression model corroborated this result by showing that seasonal fluctuations in air temperature, soil temperature, WFPS (Figure 3b), and NH_4^+ all correlated with N_2O flux (*P* < 0.05). Air temperature explained the largest proportion of variance in the data (26.2 %; negative trend), followed by soil temperature (15.5 %; positive trend), WFPS (13.7 %; negative trend), and resin-extractable NH_4^+ flux (11.6 %; negative trend).

5.4 Water-filled pore space manipulation

^{15}N-N_2O and ^{15}N-N_2 fluxes showed a biphasic response (Limmer and Steele, 1982), with significantly different flux rates in the first 24 hours of incubation compared to the later period of incubation (i.e. 24-48 hours). Flux of ^{15}N-N_2O, and ^{15}N-N_2 were therefore divided into early (0-24 hours) and late (24-48 hours) phase flux.

5.4.1 Role of nitrification and nitrate reduction in N_2O production

The ^{15}N flux data indicates that nitrate reduction (i.e. denitrification) was the dominant source of N_2O from these soils, while nitrification was only a minor contributor to ^{15}N-N_2O production (Supplementary Online Materials Figure S1). The ^{15}N-N_2O and ^{15}N-N_2 fluxes were analyzed using a full factorial ANOVA on Box-Cox transformed data with habitat, moisture level, form of ^{15}N-label added (i.e. $^{15}NH_4{}^{15}NO_3$ or $^{14}NH_4{}^{15}NO_3$), incubation phase, and all their interaction terms as independent variables. Notably, this analysis revealed that the form of ^{15}N-label added (i.e. ^{15}N-$NH_4{}^{15}N$-NO_3 or ^{14}N-$NH_4{}^{15}N$-NO_3) did not significantly alter ^{15}N-N_2O

flux, indicating that production of $^{15}N\text{-}N_2O$ from nitrification was weak to negligible (Supplementary Online Materials Figure S1). In order to simplify our statistical analyses, all subsequent analyses were performed using only habitat, moisture level, incubation phase, and their interaction terms as independent variables. For these tests, which are described below, the "total" flux of $^{15}N\text{-}N_2O$ or $^{15}N\text{-}N_2$ represents gas produced by both nitrification and nitrate reduction.

5.4.2 $^{15}N\text{-}N_2O$ flux

For the total $^{15}N\text{-}N_2O$ flux data, we used a full factorial ANOVA on Box-Cox transformed data with habitat, moisture level, incubation phase, and all their interactions as independent variables. We found that moisture level, habitat by incubation phase, and habitat by moisture by incubation phase were significantly related to $^{15}N\text{-}N_2O$ flux (ANOVA, $F_{31, 321}$ = 3.06, $P < 0.0001$; Figure 4; Supplementary Online Materials Table S2A). Of the three main factors (i.e. habitat, moisture level, incubation phase), moisture level was the dominant control on $^{15}N\text{-}N_2O$ flux (Supplementary Online Materials Table S2A). The highest $^{15}N\text{-}N_2O$ flux was observed in the 90 % WFPS (42 ± 9 ng $N_2O\text{-}^{15}N\ g^{-1}\ d^{-1}$) and 50 % WFPS (29 ± 10 ng $N_2O\text{-}^{15}N\ g^{-1}\ d^{-1}$) treatments, and the lowest flux in the 30 % (3 ± 1 ng $N_2O\text{-}^{15}N\ g^{-1}\ d^{-1}$) and 70 % (7 ± 2 ng $N_2O\text{-}^{15}N\ g^{-1}\ d^{-1}$) treatments (Fisher's LSD, $P < 0.05$; Figure 4). The habitat by incubation phase interaction indicated that some habitats showed different flux rates during early and late phases of the incubation (Figure 4). Premontane and lower montane forest showed statistically similar $^{15}N\text{-}N_2O$ flux during early and late incubation phases. Upper montane forest mineral layer soils showed a significant increase in $^{15}N\text{-}N_2O$ flux from early to late incubation phases (5 ± 2 ng $N_2O\text{-}^{15}N\ g^{-1}\ d^{-1}$ versus 42 ± 13 ng $N_2O\text{-}^{15}N\ g^{-1}\ d^{-}1$; t-Test, $P <$ 0.003), while montane grasslands showed a significant decrease in $^{15}N\text{-}N_2O$ flux from early to late incubation phases (60 ± 23 ng $N_2O\text{-}^{15}N\ g^{-1}\ d^{-1}$ versus 6 ± 9 ng $N_2O\text{-}^{15}N\ g^{-1}\ d^{-1}$, respectively; t-Test, $P < 0.02$). The habitat by moisture by incubation phase effect stems from complex and varying responses of soils from different habitats to differences in moisture level and incubation phase (Figure 4).

5.4.3 $^{15}N^{-}N_2$ flux

For the total $^{15}N\text{-}N_2$ flux data, we used a full factorial ANOVA on Box-Cox transformed data with habitat, moisture level, incubation phase, and all their interactions as independent

590 variables. We found that all of the main factors and their interaction terms were statistically
591 significant (ANOVA, $F_{31, 317}$ = 14.20, P < 0.0001; Supplementary Online Materials Table S2B).
592 Of the three main factors, habitat was the dominant control on ^{15}N-N_2 flux (Supplementary
593 Online Materials Table S2B). Lower montane forest showed the highest ^{15}N-N_2 flux (694 ± 83
594 ng N_2-^{15}N g^{-1} d^{-1}); premontane forest and upper montane forest mineral layer soil showed
595 intermediate levels of flux (326 ± 53 and 171 ± 20 ng N_2-^{15}N g^{-1} d^{-1}, respectively); and
596 montane grassland soil showed the lowest flux (123 ± 23 ng N_2O-^{15}N g^{-1} d^{-1}) (Fisher's LSD, P <
597 0.05; Figure 4). Moisture played a secondary role in regulating ^{15}N-N_2 flux (Supplementary
598 Online Materials Table S2B), with only the 90 % treatment had significantly higher flux than
599 the other treatments (90 % WFPS treatment: 437 ± 77 ng N_2-^{15}N g^{-1} d^{-1}; pooled average for
600 all other treatments: 294 ± 28 ng N_2-^{15}N g^{-1} d^{-1}) (Fisher's LSD, P < 0.05). Incubation phase was
601 the least important control on ^{15}N-N_2 flux, with slightly greater flux of ^{15}N-N_2 during the late
602 compared to the early phase of the incubations (373 ± 44 ng N_2-^{15}N g^{-1} d^{-1} versus 288 ± 37 ng
603 N_2-^{15}N g^{-1} d^{-1}) (t-Test, P < 0.07). The habitat by moisture level interaction indicates that flux
604 from different habitats showed varying moisture responses (Figure 4). For example, ^{15}N-N_2
605 flux from premontane forest and upper montane forest mineral layer soil showed no
606 responses to moisture. In contrast, for lower montane forest, flux was greatest for the 90 %
607 WFPS treatment (1,365 ± 201 ng N_2-^{15}N g^{-1} d^{-1}), lowest for the 70 % WFPS treatment (257 ±
608 128 ng N_2-^{15}N g^{-1} d^{-1}), and at intermediate levels for the 30 and 50 % WFPS treatments (664 ±
609 131 and 492 ± 79 ng N_2-^{15}N g^{-1} d^{-1}, respectively) (Fisher's LSD, P < 0.05). The pattern for
610 montane grassland was different again; here, only the 90 % WFPS treatment showed
611 significantly greater flux (171 ± 32 ng N_2-^{15}N g^{-1} d^{-1}) compared to the other treatments
612 (pooled average: 105 ± 29 ng N_2-^{15}N g^{-1} d^{-1}) (Fisher's LSD, P < 0.05).
613
614 **5.4.4 N_2O Yield**
615 For the N_2O yield, we used a full factorial ANOVA on Box-Cox transformed data with habitat,
616 moisture level, incubation phase, and all their interactions as independent variables. We
617 found that habitat, moisture level, habitat by moisture level, habitat by phase, and habitat
618 by moisture level by phase significantly influenced N_2O yield (ANOVA, $F_{31, 313}$ = 9.85, P <
619 0.0001; Supplementary Online Materials Table S2C). Of the three main factors, habitat was
620 the best predictor of N_2O yield (Supplementary Online Materials Table S2C). N_2O yield was
621 highest for the montane grassland (0.61 ± 0.06), lowest for lower montane forest (0.19 ±

622 0.04), while premontane forest and upper montane forest mineral layer soil showed similar
623 intermediate values (0.40 ± 0.05 and 0.42 ± 0.05, respectively) (Fisher's LSD, $P < 0.05$).
624 Moisture level explained much less of the variance in the dataset (Supplementary Online
625 Materials Table S2C); N_2O yield was highest for the 70 % WFPS treatment (0.51 ± 0.06), while
626 the 30, 50 and 90 % WFPS treatments showed statistically similar values (0.35 ± 0.05, 0.39 ±
627 0.05, and 0.36 ± 0.05, respectively) (Fisher's LSD, $P < 0.05$). For the habitat by moisture level
628 interaction, this reflects the fact that only lower montane forest and upper montane forest
629 showed differences in N_2O yield with changes in moisture level. For the lower montane
630 forest, N_2O yield was greatest in the 70 % WFPS treatment (0.51 ± 0.11), whereas the other
631 treatments were not statistically different from each other (pooled average: 0.09 ± 0.03)
632 (Fisher's LSD, $P < 0.05$). Upper montane forest mineral layer soil showed the highest N_2O
633 yield for the 90 % treatment (0.72 ± 0.08), lowest yield for the 30 % WFPS treatment (0.20 ±
634 0.09), and intermediate N_2O yields for the 50 and 70 % WFPS treatments (0.29 ± 0.09 and
635 0.50 ± 0.11, respectively) (Fisher's LSD, $P < 0.05$). For the habitat by incubation phase
636 interaction, this reflects the fact that upper montane forest mineral layer soil showed an
637 increase in N_2O yield from early to late phase, while montane grassland showed a decrease
638 in N_2O yield from early to late phase. The habitat by moisture level by incubation phase
639 interaction reflects the complex and varied responses of soils from different habitats to
640 changes in moisture level and incubation phase (Figure 4).
641
642 **5.5 Litter manipulation experiment**
643 In order to investigate the relationship between leaf litter input rates and N_2O flux, we used
644 a Generalized Linear Model (GLM) and an ANCOVA that included habitat, litter treatment,
645 season, WFPS, litter input rate, litter C input rate, litter N input rate, soil temperature and air
646 temperature as independent variables. The analysis was also repeated using ANCOVA on
647 Box-Cox transformed data. Both analyses revealed no significant statistical relationship
648 between N_2O flux and any of these environmental variables, with the exception of soil
649 temperature, which showed only a weak positive relationship to N_2O flux when the data was
650 analysed using the GLM ($P < 0.05$). This relationship was not detected using ANCOVA.
651 Bivariate regression of soil temperature against N_2O flux indicated that the relationship was
652 relatively weak, with $r^2 = 0.01$ ($P < 0.05$).
653

654 **5.6 Nitrate addition experiment**

655 ^{15}N-N_2O and ^{15}N-N_2 fluxes showed a biphasic response (Limmer and Steele, 1982), with
656 significantly different flux rates in the first 24 hours of incubation compared to the later
657 period of incubation (i.e. 24-48 hours). Flux of ^{15}N-N_2O, and ^{15}N-N_2 were therefore divided
658 into early (0-24 hours) and late (24-48 hours) phase flux.

659

660 **5.6.1 ^{15}N-N_2O flux**

661 For the ^{15}N-N_2O flux data, we used a full factorial ANOVA on Box-Cox transformed data with
662 habitat, N addition level, incubation phase, and all their interaction terms as independent
663 variables. Habitat, incubation phase, and the habitat by incubation phase interaction all
664 significantly influenced ^{15}N-N_2O flux (ANOVA, $F_{29,\ 149} = 5.67$, $P < 0.0001$; Figure 5;
665 Supplementary Online Materials Table S3A). Notably, N addition level did not significantly
666 influence ^{15}N-N_2O flux. Of the three main factors (i.e. habitat, N addition level, incubation
667 phase), habitat was the best predictor of ^{15}N-N_2O flux, explaining a largest proportion of the
668 variance (Supplementary Online Materials Table S3A). Upper montane forest organic layer
669 soils showed the highest flux (238 ± 160 ng N_2O-^{15}N g^{-1} d^{-1}), lower montane (179 ± 48 ng
670 N_2O-^{15}N g^{-1} d^{-1}) and premontane (86 ± 16 ng N_2O-^{15}N g^{-1} d^{-1}) forest showed intermediate flux,
671 while montane grasslands (11 ± 4 ng N_2O-^{15}N g^{-1} d^{-1}) and upper montane forest mineral layer
672 soils (0.06 ± 0.01 ng N_2O-^{15}N g^{-1} d^{-1}) showed the lowest flux (Fisher's LSD, $P < 0.05$). The
673 effect of incubation phase was attributable to significantly greater ^{15}N-N_2O flux during the
674 late compared to early incubation phases (164 ± 66 ng N_2O-^{15}N g^{-1} d^{-1} versus 42 ± 11 ng N_2O-
675 ^{15}N g^{-1} d^{-1}; t-Test, $P < 0.05$; Figure 5). The habitat by incubation phase interaction was caused
676 by some habitats showing higher flux in certain incubation phases than others (Figure 5).
677 During the early phase, lower montane and premontane forests collectively showed the
678 highest flux (Figure 5; Fisher's LSD, $P < 0.05$). In contrast, during the late incubation phase,
679 upper montane forest organic layer soils, lower montane forest, and premontane forest now
680 showed the highest flux (Figure 5; Fisher's LSD, $P < 0.05$).

681

682 **5.6.2 ^{15}N-N_2 flux**

683 For the ^{15}N-N_2 flux data, we used a full factorial ANOVA on Box-Cox transformed data with
684 habitat, N addition level, incubation phase, and all their interaction terms as independent
685 variables. Only habitat significantly influenced flux, while other terms were not significant

(ANOVA, $F_{29, 149}$ = 1.66, P < 0.05; Figure 5; Supplementary Online Materials Table S3B). Lower montane and upper montane forest organic layer soils showed the highest flux (472 ± 139 and 576 ± 117 ng N_2-^{15}N g^{-1} d^{-1}, respectively), while all other habitats showed similar flux rates (105 ± 19 ng N_2-^{15}N g^{-1} d^{-1}) (Fisher's LSD, P < 0.05; Figure 5).

5.6.3 N_2O Yield

For the N_2O yield, we used a full factorial ANOVA on Box-Cox transformed data with habitat, N addition level, incubation phase (i.e. early versus late), and all their interaction terms as independent variables. We found that none of these factors predicted N_2O yield (ANOVA, $F_{29, 149}$ = 0.75, P > 0.82; Supplementary Online Materials Table S3C). The overall mean N_2O yield for the pooled dataset was 0.53 ± 0.04.

6. Discussion

6.1 Effects of seasonality and soil moisture on N_2O flux

Nitrous oxide flux in the Kosñipata Valley showed weak seasonality, with greater N_2O flux during the dry season compared to the wet season. This regional trend was consistent with results from our prior study, and was principally driven by strong seasonality in N_2O flux from lower montane forest (Teh et al., 2014). In contrast, other habitats showed little or no seasonal variation in N_2O flux. This weak seasonality in N_2O flux across the Kosñipata Valley probably stems from relatively modest variation in environmental variables among seasons (Table 3), in accordance with observations from elsewhere in the Andes (Baldos et al., 2015;Müller et al., 2015;Wolf et al., 2011). For example, while soil moisture (i.e. WFPS) varied significantly between seasons in the dataset as a whole, the absolute difference in WFPS between dry season and wet season were relatively small (i.e. 7.4 %). Indeed, some habitats showed much smaller variations in soil moisture, such as premontane forest and montane grassland that showed no significant seasonal variation in WFPS whatsoever (Table 3).

One critical factor contributing to these weak seasonal trends in N_2O flux is the atypical response of N_2O flux to changes in soil moisture. Nitrous oxide flux showed a weak but negative correlation with WFPS in the field dataset (r^2= 0.01, P <0.06 for the pooled dataset),

718 rather than following a curvilinear pattern predicted by denitrification theory (Firestone and
719 Davidson, 1989;Firestone et al., 1980;Weier et al., 1993;Davidson, 1991). Likewise, in our soil
720 moisture manipulation experiments, nitrification made a minor contribution to N_2O
721 production, irrespective of soil moisture content (Supplementary Online Materials Figure
722 S1). This finding is contrary to theoretical predictions of N_2O production by ammonia-
723 oxidizing bacteria (AOB), where N_2O production from ammonia-oxidation is thought to make
724 an important contribution to N_2O flux at lower soil moisture contents (i.e. 30-60 % WFPS)
725 (Firestone and Davidson, 1989;Firestone et al., 1980;Weier et al., 1993;Davidson, 1991). At
726 higher soil moisture contents (i.e. >60 % WFPS), N_2O flux showed a non-linear response to
727 increasing WFPS, with two distinct peaks in N_2O flux at 90 and 50 % WFPS (Figure 4).
728 Collectively, these findings suggest that the role of soil moisture in regulating N_2O flux is
729 more complex than predicted by existing theory, falsifying our first two hypotheses.
730
731 What could explain these unexpected trends? We believe that these patterns occurred due
732 to the complex interplay between environmental conditions and the microbial processes
733 that produce N_2O in soil (i.e. ammonia oxidation by archaea, ammonia oxidation by bacteria,
734 denitrification, dissimilatory nitrate reduction to ammonium). We suspect that the action of
735 lesser-known microbial processes, such as oxidation of ammonia by archaea and
736 dissimilatory nitrate reduction to ammonium (DNRA), may explain the divergence from
737 theoretical norms. Our expectations of how N_2O production should respond to variations in
738 soil moisture are predicated on the assumption that N_2O is produced almost exclusively by
739 AOB and denitrifying bacteria, with the former operating at lower soil moisture content (i.e.
740 30-60 % WFPS) and the latter at higher soil moisture content (i.e. >60 % WFPS) (Firestone
741 and Davidson, 1989;Firestone et al., 1980;Weier et al., 1993;Davidson, 1991). More recent
742 advances in soil N research, however, have highlighted the importance of other microbial
743 taxa or processes, not previously considered in conceptual or process-based models. For
744 example, recent work in acidic soils have demonstrated that ammonia oxidizing archaea
745 (AOA) play a more important role than AOB in ammonia oxidation, but produce significantly
746 less N_2O due to differences in metabolism (Hink et al., 2016;Prosser and Nicol, 2008).
747 Likewise, under higher soil moisture conditions (>60 % WFPS), DNRA – a process that
748 produces substantially less N_2O than denitrification and which also competes for NO_3^- with
749 denitrification – can dominate nitrate reduction, depending on redox conditions and the

750 relative availability of labile C and N (Morley and Baggs, 2010;Pett-Ridge and Firestone,
751 2005;Silver et al., 2001;Baldos et al., 2015;Müller et al., 2015). Thus, given the low pH of the
752 soils in Kosñipata Valley (Table 1), it is likely that AOA dominate ammonia oxidation at lower
753 levels of soil moisture, explaining the negligible amounts of N_2O produced from nitrification
754 in the 30 and 50 % WFPS treatments. As soils become wetter, the non-linear response of
755 N_2O flux to increasing soil moisture may reflect competition for substrates (e.g. NO_3^-,
756 reducing equivalents) between DNRA and denitrification (Morley and Baggs, 2010;Silver et
757 al., 2001), or may indicate that DNRA is making a larger contribution to N_2O flux than
758 denitrification (Streminska et al., 2012).
759
760 These findings are important and noteworthy, given that climatically-driven variations in soil
761 moisture content are thought to be one of the dominant drivers for N_2O flux in the
762 seasonally dry tropics (Davidson, 1991;Firestone and Davidson, 1989;Groffman et al.,
763 2009;Davidson and Verchot, 2000;Teh et al., 2014;van Lent et al., 2015;Werner et al., 2007).
764 Moreover, similar results from comparable research sites in the Ecuadorian Andes lend
765 credence to our claims (Baldos et al., 2015;Müller et al., 2015). For example, Müller et al.
766 (2015) found that nitrification produced little or no N_2O in acidic Ecuadorian soils, in
767 agreement with findings from in this study. Likewise, ^{15}N isotope pool dilution experiments,
768 in comparable habitats and elevations to our own, revealed that DNRA played a significant
769 role in nitrate reduction, supporting the notion that DNRA may represent a substantial sink
770 for NO_3^- in Peruvian soils (Baldos et al., 2015;Müller et al., 2015). Existing process-based
771 models, which are used to construct bottom-up emissions inventories for the tropics
772 (Werner et al., 2007), often assume that N_2O is derived primarily from AOB and
773 denitrification, with moisture response curves based on existing theoretical relationships (Li
774 et al., 2000;Werner et al., 2007;Smith et al., 2007). However, if these more “normative” soil
775 moisture response curves are inapplicable to montane tropical ecosystems, due to the
776 activity of AOA and DNRA, then a re-conceptualisation of the soil moisture-N_2O flux
777 relationship may be required. Moreover, if weak seasonality or aseasonality in N_2O flux is
778 the norm in Andean ecosystems (Müller et al., 2015;Wolf et al., 2011), then this finding may
779 have wider implications for understanding spatial or temporal trends in regional
780 atmospheric budgets (Kort et al., 2011;Nevison et al., 2004;Nevison et al., 2007;Saikawa et
781 al., 2014).

782

783 **6.2 Role of substrate limitation in regulating N_2O flux**

784 In accordance with our earlier work (Teh et al., 2014) and research conducted in analogous
785 ecosystems in Ecuador (Baldos et al., 2015;Müller et al., 2015;Wolf et al., 2011), we found
786 strong evidence that N_2O flux was constrained by the availability of NO_3^-, partially supporting
787 our third hypothesis. In contrast, N_2O flux was unresponsive to short-term changes in labile
788 organic matter (i.e. leaf litter-fall) inputs, indicating that N_2O flux and nitrate reduction were
789 not C limited. This latter result is significant for modelling and extrapolating N_2O flux from
790 these habitats, because many process-based models assume that N cycling and turnover of
791 labile organic matter are intimately linked through processes such as litter production and
792 decomposition (Li et al., 2000;Werner et al., 2007;Smith et al., 2007).

793

794 Evidence for NO_3^- limitation of N_2O flux comes from both our field and laboratory data, and
795 suggests that "habitat" may be a good proxy for NO_3^- availability and N_2O flux because these
796 two variables co-vary with habitat. For example, we observed an inverse trend in field N_2O
797 flux, with premontane forest showing significantly greater flux than the other habitats
798 elevation (Table 3, Figure 2a). This inverse trend was also reflected in the resin-extractable
799 NO_3^- flux measured in the field and the ^{15}N-N_2O flux measured in the NO_3^- addition
800 experiment in the laboratory (Figure 2c, 5a). Furthermore, the behaviour of the ^{15}N-NO_3^-
801 amended soils during the early (≤24 hours) and late (>24 hours) phases of the incubation
802 experiment suggest that soils from more N-poor habitats (i.e. those with lower rates of
803 resin-extractable NO_3^- flux; Table 3, Figure 2c) showed a greater proportional increase in ^{15}N-
804 N_2O flux following NO_3^- addition than N-rich habitats (i.e. those with higher rates of resin-
805 extractable NO_3^- flux; Table 3, Figure 2c), suggesting that ^{15}N-N_2O flux was more NO_3^- limited
806 in N-poor soils (Figure 5). Soils from the upper montane forest organic layer, montane
807 grasslands, and upper montane forest mineral layer showed the lowest ^{15}N-N_2O flux during
808 the early phase of soil incubation, but the greatest proportional increase in flux during the
809 late phase of soil incubation, rising by a factor of 59, five, and two, respectively. In contrast,
810 lower montane and premontane forest soils showed the smallest proportional increase in
811 the late phase of soil incubation (i.e. 1.7 times increase). Last, the relatively low N_2O yield
812 observed in our soil moisture manipulations is thought to be broadly indicative of low NO_3^-
813 conditions (i.e. <0.42 for forested habitats; Table 4), further supporting the notion that N_2O

flux in this region is generally NO_3^- limited (Schlesinger, 2009;Fang et al., 2015;Weier et al., 1993).

Interestingly, we found no evidence that these soils responded to short-term increases in NO_3^- availability, at least within the concentration range used for the experiments described here. ^{15}N-N_2O flux, ^{15}N-N_2 flux, and N_2O yield were not directly influenced by the amount of ^{15}N-NO_3^- added (Figure 5). Rather, ANCOVA suggests that ^{15}N-N_2O and ^{15}N-N_2 fluxes were better-predicted by habitat. N_2O yield, normally a sensitive indicator of NO_3^- availability (Blackmer and Bremner, 1978;Weier et al., 1993;Parton et al., 1996), showed no immediate response to the amount of ^{15}N-NO_3^- added, nor any of the other explanatory variables. One explanation for this, consistent with the notion that N_2O flux is NO_3^- limited, is that nitrate-reducing microbes in these soils may have a relatively low half-saturation constant (K_m) for NO_3^-, and effectively utilize NO_3^- whenever concentrations increase above baseline (i.e. non-limiting) levels (Holtan-Hartwig et al., 2000). As a consequence, we may be unable to differentiate among NO_3^- treatments because the NO_3^- addition levels that we used all exceeded the K_m for these soils. This finding is also in agreement with results from long-term N fertilization studies, which suggest that substantive shifts in N_2O flux are only likely to occur after prolonged exposure to high levels of N (i.e. >1 year), rather than due to transient fluctuations in N availability (Baldos et al., 2015;Corre et al., 2010;Müller et al., 2015;Hall and Matson, 1999;Koehler et al., 2012).

6.3 Implications for annual atmospheric budgets and gaseous N loss

Montane ecosystems in the Kosñipata Valley were net sources of atmospheric N_2O, affirming our prior results (Teh et al., 2014). The flux for this multi-annual dataset was comparable to the preliminary values reported in our earlier publication, with an unweighted mean flux of 0.27 ± 0.07 mg N-N_2O m^{-2} d^{-1} observed over a 30 month period compared to 0.22 ± 0.12 mg N-N_2O m^{-2} d^{-1} recorded over a 13 month period (Teh et al., 2014). These values correspond to unweighted mean annual fluxes of 0.99 ± 0.26 kg N_2O-N ha^{-1} $year^{-1}$ and 0.80 ± 0.44 kg N_2O-N ha^{-1} $year^{-1}$, respectively. However, in order to derive more accurate estimates of the annual contribution of the Kosñipata Valley to the regional atmospheric budget of N_2O, it is necessary to account for differences in land area for different habitats and variation in the magnitude of N_2O flux between seasons. Thus, we conducted a simple weighted upscaling

exercise to more fully account for these two sources of variation (Table 4). Using the N_2O yield data from the laboratory tracer experiments, we also estimated the annual N_2 flux and total gaseous N flux, in order compare rates of gaseous N export from this region with other forested ecosystems (Fang et al., 2015;Russell and Raich, 2012;Tietema and Verstraten, 1991;Bai et al., 2012) (Table 4). We fully acknowledge that this simple approach is not as robust as bottom-up, process-based emissions inventories (Werner et al., 2007). Even so, we believe it is still useful for providing first-order approximations of annual N_2O, N_2 and total gaseous N flux.

To briefly summarize our methodology, our first step was to use published surface area estimates for the different habitats in the Kosñipata Valley to derive areal fractions for each habitat (Feeley and Silman, 2010) (Table 4). Next, we multiplied the unweighted seasonal mean flux by the areal fraction for each habitat to derive area-weighted seasonal flux estimates (Table 4). We subsequently multiplied the area-weighted seasonal flux by the fraction of the year accounted for by either season, in order to produce an area-weighted and seasonally-weighted annual flux estimate for each habitat (Table 4). The final step of this process was to sum the area-weighted and seasonally-weighted flux estimates for each habitat, to drive an overall weighted flux estimate for the Kosñipata Valley as a whole (Table 4). Weighted annual estimates of N_2 flux were calculated using the N_2O yield values for each habitat as determined in our soil moisture manipulation experiment (Table 4). We elected to use mean N_2O yields for each habitat, rather than estimating N_2O yield based on soil moisture content, because ANCOVA indicated that habitat was a better predictor of N_2O yield than soil moisture, explaining a substantially greater proportion of the variance (i.e. 10 % versus only 1 % of the variance; see Supplementary Online Materials Table S2C). Total gaseous N export was estimate by calculating the sum of annual N_2O and N_2 flux. Errors for all the annual flux estimates (i.e. N_2O, N_2, total gaseous N) were propagated using standard error propagation techniques.

We determined that the Kosñipata Valley emitted approximately 1.27 ± 0.33 kg N_2O-N ha^{-1} $year^{-1}$, 3.29± 1.27 kg N_2-N ha^{-1} $year^{-1}$, and 4.57 ± 1.31 kg N ha^{-1} $year^{-1}$. Annual N_2O flux was broadly on par with our earlier estimates (i.e. 1.18 ± 0.79 kg N_2O-N ha^{-1} $year^{-1}$) (Teh et al., 2014). This estimated annual rate of flux exceeds the value for montane tropical montane

878 forests calculated by Werner et al. (2007) using a bottom-up process model (i.e. 0.5 to 1 kg
879 N_2O-N ha^{-1} $year^{-1}$), but falls within the range predicted for humid tropical forest soils more
880 generally (i.e. approximately 1-4 kg N_2O-N ha^{-1} $year^{-1}$) (van Lent et al., 2015;Werner et al.,
881 2007). Annual N_2 flux and total gaseous N flux are at the lower end of the range reported in
882 comparable studies from other ecosystems (e.g. Fang et al., 2015 reported annual gaseous
883 losses of 5.6– 30.1 kg N ha^{-1} $year^{-1}$ sampling across a broad range of temperate and tropical
884 ecosystems) (Fang et al., 2015;Russell and Raich, 2012;Tietema and Verstraten, 1991;Bai et
885 al., 2012), further supporting claims that Andean ecosystems are relatively N limited, and
886 may cycle N more conservatively than lowland forests (Baldos et al., 2015;Müller et al.,
887 2015;Wolf et al., 2011;Nottingham et al., 2015)
888
889
890 **7. Conclusions**
891 Process-based studies of N_2O flux from montane tropical ecosystems in the southern
892 Peruvian Andes affirms prior research suggesting that these ecosystems are potentially
893 important regional sources of N_2O (Teh et al., 2014). Simple weighted upscaling suggests
894 that annual N_2O flux from the Kosñipata Valley is on the order of 1.27 ± 0.33 kg N_2O-N ha^{-1}.
895 Habitat – a proxy for NO_3^- availability under field conditions – was the best predictor for N_2O
896 flux, with more N-rich habitats (i.e. premontane forest) showing significantly higher N_2O flux
897 than habitats with lower N availability (i.e. upper montane forest, montane grassland).
898 Nitrous oxide flux originated primarily from nitrate reduction rather than from nitrification,
899 probably due to low pH soil conditions which may have inhibited the activity of AOB.
900 Contrary to our prior research, we found only weak evidence for seasonal trends in field N_2O
901 flux, with the exception of lower montane forest, which showed significantly higher N_2O flux
902 during the dry season compared to the wet season. Weak seasonal trends in field N_2O flux
903 among the other montane habitats probably stems from relatively modest seasonal
904 variation in key environmental drivers (e.g. temperature, WFPS, NO_3^-), combined with a soil
905 moisture response that was complex and non-linear. Nitrous oxide flux was significantly
906 influenced by soil moisture content, but the trends in N_2O production and flux diverged from
907 theoretical norms. For example, we saw little evidence of N_2O production from ammonia-
908 oxidation, even though the field measurement (i.e. resin bags) indicate that nitrification
909 occurs. This may be due to the predominance of AOA, which produce significantly N_2O than

AOB, under the acidic conditions common in Andean soils. At higher soil moisture levels, N_2O flux increased non-linearly with WFPS, with peaks in N_2O flux at 90 and 50 % WFPS. These results suggest that the effects of water on N_2O flux are complicated by other factors, such as competition for substrates among different nitrate-reducing processes, or shifts in the amount of N_2O derived from denitrification or DNRA. Field data and substrate manipulation experiments indicated that N_2O flux was strongly limited by NO_3^-, but unconstrained by the input rate of labile organic matter (i.e. leaf litter). Nitrous oxide flux was relatively insensitive to short-term variations in NO_3^-, and was better-predicted by longer-term, time-averaged variations in NO_3^- availability.

8. Data Availability

Data for this publication are publically available from the UK Natural Environment Research Council (NERC) Centre for Environmental Data Analysis (CEDA), at the following URL: http://catalogue.ceda.ac.uk/uuid/93fdb48b713b4dbc93a28d695771312d

9. Author Contributions

TD designed the field and laboratory experiments, collected the field data, conducted the laboratory experiments, processed the samples, analysed the data, and contributed to the preparation of the manuscript. NJM contributed to the design of the laboratory experiments, assisted in the sample analysis, assisted in the analysis of the laboratory data, and contributed to the preparation of the manuscript. AJC and LPHQ assisted in the collection of the field data and processing of the field samples. EMB, PM, MR, and PS contributed to the experimental design and the preparation of the manuscript. YAT directed the research, contributed to the design of the experiments, assisted in the analysis of the field and laboratory data, and took the principal role in preparing the manuscript.

10. Acknowledgements

The authors would like to acknowledge the agencies that funded this research; the UK Natural Environment Research Council (NERC; joint grant references NE/H006583,

NE/H007849 and NE/H006753). Patrick Meir was supported by an Australian Research Council Fellowship (FT110100457). Javier Eduardo Silva Espejo, Walter Huaraca Huasco, and the ABIDA NGO provided critical fieldwork and logistical support. Angus Calder (University of St Andrews) and Vicky Munro (University of Aberdeen) provided invaluable laboratory support. Thanks to Adrian Tejedor from the Amazon Conservation Association, who provided assistance with site access and site selection at Hacienda Villa Carmen. This publication is a contribution from the Scottish Alliance for Geoscience, Environment and Society (http://www.sages.ac.uk).

11. References

Baggs, E. M., Richter, M., Hartwig, U.A., and Cadisch, G. : Nitrous oxide emissions from grass swards during the eighth year of elevated atmospheric pCO2 (Swiss FACE). , Global Change Biology 9, 1214-1222., 2003.

Bai, E., Houlton, B. Z., and Wang, Y. P.: Isotopic identification of nitrogen hotspots across natural terrestrial ecosystems, Biogeosciences, 9, 3287-3304, 10.5194/bg-9-3287-2012, 2012.

Baldos, A. P., Corre, M. D., and Veldkamp, E.: Response of N cycling to nutrient inputs in forest soils across a 1000–3000 m elevation gradient in the Ecuadorian Andes, Ecology, 96, 749-761, 10.1890/14-0295.1, 2015.

Bateman, E. J., and Baggs, E. M.: Contributions of nitrification and denitrification to N2O emissions from soils at different water-filled pore space, Biology and Fertility of Soils, 41, 379-388, 10.1007/s00374-005-0858-3, 2005.

Belyea, L. R., and Baird, A. J.: Beyond "The limits to peat bog growth'': Cross-scale feedback in peatland development, Ecological Monographs, 76, 299-322, 2006.

Blackmer, A. M., and Bremner, J. M.: Inhibitory effect of nitrate on reduction of N2O to N2 by soil microorganisms, Soil Biology and Biochemistry, 10, 187-191, http://dx.doi.org/10.1016/0038-0717(78)90095-0, 1978.

Breuer, L., Papen, H., and Butterbach-Bahl, K.: N2O emission from tropical forest soils of Australia, J. Geophys. Res.-Atmos., 105, 26353-26367, 10.1029/2000jd900424, 2000.

Corre, M. D., Veldkamp, E., Arnold, J., and Wright, S. J.: Impact of elevated N input on soil N cycling and losses in old-growth lowland and montane forests in Panama, Ecology, 91, 1715-1729, 10.1890/09-0274.1, 2010.

Davidson, E. A.: Fluxes of nitrous oxide and nitric oxide from terrestrial ecosystems, in: Microbial production and consumption of greenhouse gases: methane, nitrogen oxides, and halomethanes., edited by: Rogers, J. E., and Whitman, W. B., American Society for Microbiology, Washington D.C., 219-236, 1991.

Davidson, E. A., and Verchot, L. V.: Testing the Hole-in-the-Pipe Model of nitric and nitrous oxide emissions from soils using the TRAGNET Database, Global Biogeochemical Cycles, 14, 1035-1043, 10.1029/1999GB001223, 2000.

Eva, H. D., Belward, A. S., De Miranda, E. E., Di Bella, C. M., Gond, V., Huber, O., Jones, S., Sgrenzaroli, M., and Fritz, S.: A land cover map of South America, Global Change Biology, 10, 731-744, 10.1111/j.1529-8817.2003.00774.x, 2004.

Fang, Y., Koba, K., Makabe, A., Takahashi, C., Zhu, W., Hayashi, T., Hokari, A. A., Urakawa, R., Bai, E., Houlton, B. Z., Xi, D., Zhang, S., Matsushita, K., Tu, Y., Liu, D., Zhu, F., Wang, Z., Zhou, G., Chen, D., Makita, T., Toda, H., Liu, X., Chen, Q., Zhang, D., Li, Y., and Yoh, M.: Microbial denitrification dominates nitrate losses from forest ecosystems, Proceedings of the National Academy of Sciences, 112, 1470-1474, 10.1073/pnas.1416776112, 2015.

Feeley, K. J., and Silman, M. R.: Land-use and climate change effects on population size and extinction risk of Andean plants, Global Change Biology, 16, 3215-3222, 10.1111/j.1365-2486.2010.02197.x, 2010.

Firestone, M. K., Firestone, R. B., and Tiedge, J. M.: Nitrous oxide from soil denitrification: Factors controlling its biological production., Science, 208, 749-751, 1980.

Firestone, M. K., and Davidson, E. A.: Microbiological basis of NO and N2O production and consumption in soil, in: Exchange of Trace Gases Between Terrestrial Ecosystems and the Atmosphere, edited by: Andrae, M. O., and Schimel, D. S., John Wiley and Sons Ltd., New York, 7-21, 1989.

Girardin, C. A. J., Malhi, Y., AragÃO, L. E. O. C., Mamani, M., Huaraca Huasco, W., Durand, L., Feeley, K. J., Rapp, J., Silva-Espejo, J. E., Silman, M., Salinas, N., and Whittaker, R. J.: Net primary productivity allocation and cycling of carbon along a tropical forest elevational transect in the Peruvian Andes, Global Change Biology, 16, 3176-3192, 10.1111/j.1365-2486.2010.02235.x, 2010.

1004 Groffman, P. M., Butterbach-Bahl, K., Fulweiler, R. W., Gold, A. J., Morse, J. L., Stander, E. K.,
1005 Tague, C., Tonitto, C., and Vidon, P.: Challenges to incorporating spatially and temporally
1006 explicit phenomena (hotspots and hot moments) in denitrification models, Biogeochemistry,
1007 93, 49-77, 10.1007/s10533-008-9277-5, 2009.
1008 Hall, S. J., and Matson, P. A.: Nitrogen oxide emissions after nitrogen additions in tropical
1009 forests, Nature, 400, 152-155, 1999.
1010 Hink, L., Nicol, G. W., and Prosser, J. I.: Archaea produce lower yields of N2O than bacteria
1011 during aerobic ammonia oxidation in soil, Environ. Microbiol., n/a-n/a, 10.1111/1462-
1012 2920.13282, 2016.
1013 Hirsch, A. I., Michalak, A. M., Bruhwiler, L. M., Peters, W., Dlugokencky, E. J., and Tans, P. P.:
1014 Inverse modeling estimates of the global nitrous oxide surface flux from 1998-2001, Global
1015 Biogeochemical Cycles, 20, 1-17, Gb1008
1016 10.1029/2004gb002443, 2006.
1017 Holtan-Hartwig, L., Dorsch, P., and Bakken, L. R.: Comparison of denitrifying communities in
1018 organic soils: kinetics of NO3- and N2O reduction, Soil Biol. Biochem., 32, 833-843,
1019 10.1016/s0038-0717(99)00213-8, 2000.
1020 Huang, J., Golombek, A., Prinn, R., Weiss, R., Fraser, P., Simmonds, P., Dlugokencky, E. J.,
1021 Hall, B., Elkins, J., Steele, P., Langenfelds, R., Krummel, P., Dutton, G., and Porter, L.:
1022 Estimation of regional emissions of nitrous oxide from 1997 to 2005 using multinetwork
1023 measurements, a chemical transport model, and an inverse method, J. Geophys. Res.-
1024 Atmos., 113, 1-19, D17313
1025 10.1029/2007jd009381, 2008.
1026 Jones, S. P., Diem, T., Huaraca Quispe, L. P., Cahuana, A. J., Reay, D. S., Meir, P., and Teh, Y.
1027 A.: Drivers of atmospheric methane uptake by montane forest soils in the southern Peruvian
1028 Andes, Biogeosciences, 13, 4151-4165, 10.5194/bg-13-4151-2016, 2016.
1029 Koehler, B., Corre, M. D., Steger, K., Well, R., Zehe, E., Sueta, J. P., and Veldkamp, E.: An in-
1030 depth look into a tropical lowland forest soil: nitrogen-addition effects on the contents of
1031 N2O, CO2 and CH4 and N2O isotopic signatures down to 2-m depth, Biogeochemistry, 111,
1032 695-713, 10.1007/s10533-012-9711-6, 2012.
1033 Kort, E. A., Patra, P. K., Ishijima, K., Daube, B. C., Jimenez, R., Elkins, J., Hurst, D., Moore, F. L.,
1034 Sweeney, C., and Wofsy, S. C.: Tropospheric distribution and variability of N2O: Evidence for
1035 strong tropical emissions, Geophys. Res. Lett., 38, 5, 10.1029/2011gl047612, 2011.

Li, C., Aber, J., Stange, F., Butterbach-Bahl, K., and Papen, H.: A process-oriented model of N2O and NO emissions from forest soils: 1. Model development, Journal of Geophysical Research: Atmospheres, 105, 4369-4384, 10.1029/1999JD900949, 2000.

Limmer, A. W., and Steele, K. W.: Denitrification potentials: Measurement of seasonal variation using a short-term anaerobic incubation technique, Soil Biology and Biochemistry, 14, 179-184, http://dx.doi.org/10.1016/0038-0717(82)90020-7, 1982.

Livingston, G., and Hutchinson, G.: Chapter 2: Enclosure-based measurement of trace gas exchange: applications and sources of error., in: Biogenic Trace Gases: Measuring Emissions from Soil and Water., edited by: Matson, P., Harriss, RC, Blackwell Science Ltd, Cambridge, MA, USA, 14-51, 1995.

Malhi, Y., Silman, M., Salinas, N., Bush, M., Meir, P., and Saatchi, S.: Introduction: Elevation gradients in the tropics: laboratories for ecosystem ecology and global change research, Global Change Biology, 16, 3171-3175, 10.1111/j.1365-2486.2010.02323.x, 2010.

Morley, N., and Baggs, E. M.: Carbon and oxygen controls on N2O and N-2 production during nitrate reduction, Soil Biol. Biochem., 42, 1864-1871, 10.1016/j.soilbio.2010.07.008, 2010.

Moser, G., Leuschner, C., Hertel, D., Graefe, S., Soethe, N., and Iost, S.: Elevation effects on the carbon budget of tropical mountain forests (S Ecuador): the role of the belowground compartment, Global Change Biology, 17, 2211-2226, 10.1111/j.1365-2486.2010.02367.x, 2011.

Müller, A. K., Matson, A. L., Corre, M. D., and Veldkamp, E.: Soil N2O fluxes along an elevation gradient of tropical montane forests under experimental nitrogen and phosphorus addition, Frontiers in Earth Science, 3, 66, 2015.

Nevison, C. D., Lueker, T. J., and Weiss, R. F.: Quantifying the nitrous oxide source from coastal upwelling, Global Biogeochemical Cycles, 18, 24, Gb1018 10.1029/2003gb002110, 2004.

Nevison, C. D., Mahowald, N. M., Weiss, R. F., and Prinn, R. G.: Interannual and seasonal variability in atmospheric N2O, Global Biogeochemical Cycles, 21, GB3017, 10.1029/2006GB002755, 2007.

Nottingham, A. T., Turner, B. L., Whitaker, J., Ostle, N. J., McNamara, N. P., Bardgett, R. D., Salinas, N., and Meir, P.: Soil microbial nutrient constraints along a tropical forest elevation gradient: a belowground test of a biogeochemical paradigm, Biogeosciences, 12, 6071-6083, 10.5194/bg-12-6071-2015, 2015.

1068 Parton, W. J., Mosier, A. R., Ojima, D. S., Valentine, D. W., Schimel, D. S., Weier, K., and
1069 Kulmala, A. E.: Generalized model for N2 and N2O production from nitrification and
1070 denitrification, Global Biogeochemical Cycles, 10, 401-412, 10.1029/96GB01455, 1996.
1071 Pedersen, A. R., Petersen, S. O., and Schelde, K.: A comprehensive approach to soil-
1072 atmosphere trace-gas flux estimation with static chambers, European Journal of Soil Science,
1073 61, 888-902, 10.1111/j.1365-2389.2010.01291.x, 2010.
1074 Pett-Ridge, J., and Firestone, M. K.: Redox fluctuation structures microbial communities in a
1075 wet tropical soil, Appl. Environ. Microbiol., 71, 6998-7007, 10.1128/aem.71.11.6998-
1076 7007.2005, 2005.
1077 Potter, C. S., Matson, P. A., Vitousek, P. M., and Davidson, E. A.: Process modeling of controls
1078 on nitrogen trace gas emissions from soils worldwide, Journal of Geophysical Research:
1079 Atmospheres, 101, 1361-1377, 10.1029/95JD02028, 1996.
1080 Prosser, J. I., and Nicol, G. W.: Relative contributions of archaea and bacteria to aerobic
1081 ammonia oxidation in the environment, Environ. Microbiol., 10, 2931-2941, 10.1111/j.1462-
1082 2920.2008.01775.x, 2008.
1083 Pumpanen, J., Kolari, P., Ilvesniemi, H., Minkkinen, K., Vesala, T., Niinistö, S., Lohila, A.,
1084 Larmola, T., Morero, M., Pihlatie, M., Janssens, I., Yuste, J. C., Grünzweig, J. M., Reth, S.,
1085 Subke, J.-A., Savage, K., Kutsch, W., Østreng, G., Ziegler, W., Anthoni, P., Lindroth, A., and
1086 Hari, P.: Comparison of different chamber techniques for measuring soil CO2 efflux, Agric.
1087 For. Meteorol., 123, 159-176, http://dx.doi.org/10.1016/j.agrformet.2003.12.001, 2004.
1088 Russell, A. E., and Raich, J. W.: Rapidly growing tropical trees mobilize remarkable amounts
1089 of nitrogen, in ways that differ surprisingly among species, Proceedings of the National
1090 Academy of Sciences, 109, 10398-10402, 10.1073/pnas.1204157109, 2012.
1091 Saikawa, E., Schlosser, C. A., and Prinn, R. G.: Global modeling of soil nitrous oxide emissions
1092 from natural processes, Global Biogeochemical Cycles, 27, 972-989, 10.1002/gbc.20087,
1093 2013.
1094 Saikawa, E., Prinn, R. G., Dlugokencky, E., Ishijima, K., Dutton, G. S., Hall, B. D., Langenfelds,
1095 R., Tohjima, Y., Machida, T., Manizza, M., Rigby, M., O'Doherty, S., Patra, P. K., Harth, C. M.,
1096 Weiss, R. F., Krummel, P. B., van der Schoot, M., Fraser, P. J., Steele, L. P., Aoki, S., Nakazawa,
1097 T., and Elkins, J. W.: Global and regional emissions estimates for N2O, Atmospheric
1098 Chemistry and Physics, 14, 4617-4641, 10.5194/acp-14-4617-2014, 2014.

1099 Schlesinger, W. H.: On the fate of anthropogenic nitrogen, Proceedings of the National
1100 Academy of Sciences, 106, 203-208, 10.1073/pnas.0810193105, 2009.
1101 Silver, W. L., Herman, D. J., and Firestone, M. K. S.: Dissimilatory Nitrate Reduction to
1102 Ammonium in Upland Tropical Forest Soils., Ecology, 82, 2410-2416, 2001.
1103 Smith, P., Smith, J. U., Flynn, H., Killham, K., Rangel-Castro, I., Foereid, B., Aitkenhead, M.,
1104 Chapman, S., Towers, W., Bell, J., Lumsdon, D., Milne, R., Thomson, A., Simmons, I., Skiba, U.,
1105 Reynolds, B., Evans, C., Frogbrook, Z., Bradley, I., Whitmore, A., and Falloon, P.: ECOSSE:
1106 Estimating Carbon in Organic Soils - Sequestration and Emissions. Final Report., Scottish
1107 Executive Environment and Rural Affairs Department Report, 166 pp., 2007.
1108 Streminska, M. A., Felgate, H., Rowley, G., Richardson, D. J., and Baggs, E. M.: Nitrous oxide
1109 production in soil isolates of nitrate-ammonifying bacteria, Environ. Microbiol. Rep., 4, 66-
1110 71, 10.1111/j.1758-2229.2011.00302.x, 2012.
1111 Subler, S., Blair, J. M., and Edwards, C. A.: Using anion-exchange membranes to measure soil
1112 nitrate availability and net nitrification, Soil Biology and Biochemistry, 27, 911-917,
1113 http://dx.doi.org/10.1016/0038-0717(95)00008-3, 1995.
1114 Team, R. C.: A language and environment for statistical computing, R Foundation for
1115 Statistical Computing, Vienna, Austria, 2012.
1116 Teh, Y. A., Diem, T., Jones, S., Huaraca Quispe, L. P., Baggs, E., Morley, N., Richards, M.,
1117 Smith, P., and Meir, P.: Methane and nitrous oxide fluxes across an elevation gradient in the
1118 tropical Peruvian Andes, Biogeosciences, 11, 2325-2339, 10.5194/bg-11-2325-2014, 2014.
1119 Templer, P. H., Lovett, G. M., Weathers, K. C., Findlay, S. E., and Dawson, T. E.: Influence of
1120 tree species on forest nitrogen retention in the Catskill Mountains, New York, USA,
1121 Ecosystems, 8, 1-16, 10.1007/s10021-004-0230-8, 2005.
1122 Tietema, A., and Verstraten, J. M.: Nitrogen cycling in an acid forest ecosystem in the
1123 Netherlands under increased atmospheric nitrogen input, Biogeochemistry, 15, 21-46,
1124 10.1007/bf00002807, 1991.
1125 van Lent, J., Hergoualc'h, K., and Verchot, L. V.: Reviews and syntheses: Soil N2O and NO
1126 emissions from land use and land use change in the tropics and subtropics: a meta-analysis,
1127 Biogeosciences, 15, 7299-7313 pp., 2015.
1128 Varner, R. K., Keller, M., Robertson, J. R., Dias, J. D., Silva, H., Crill, P. M., McGroddy, M., and
1129 Silver, W. L.: Experimentally induced root mortality increased nitrous oxide emission from
1130 tropical forest soils, Geophys. Res. Lett., 30, n/a-n/a, 10.1029/2002GL016164, 2003.

Veldkamp, E., Purbopuspito, J., Corre, M. D., Brumme, R., and Murdiyarso, D.: Land use change effects on trace gas fluxes in the forest margins of Central Sulawesi, Indonesia, Journal of Geophysical Research-Biogeosciences, 113, 1-11, G02003 10.1029/2007jg000522, 2008.

Weier, K. L., Doran, J. W., Power, J. F., and Walters, D. T.: Denitrification and the denitrogen nitrous oxide ratio as affected by soil water, available carbon, and nitrate, Soil Sci. Soc. Am. J., 57, 66-72, 1993.

Werner, C., Butterbach-Bahl, K., Haas, E., Hickler, T., and Kiese, R.: A global inventory of N2O emissions from tropical rainforest soils using a detailed biogeochemical model, Global Biogeochemical Cycles, 21, 1-18, Gb3010 10.1029/2006gb002909, 2007.

Wolf, K., Veldkamp, E., Homeier, J., and Martinson, G. O.: Nitrogen availability links forest productivity, soil nitrous oxide and nitric oxide fluxes of a tropical montane forest in southern Ecuador, Global Biogeochemical Cycles, 25, GB4009, 10.1029/2010GB003876, 2011.

Wolf, K., Flessa, H., and Veldkamp, E.: Atmospheric methane uptake by tropical montane forest soils and the contribution of organic layers, Biogeochemistry, 111, 469-483, 10.1007/s10533-011-9681-0, 2012.

Zimmermann, M., Meir, P., Bird, M., Malhi, Y., and Ccahuana, A.: Litter contribution to diurnal and annual soil respiration in a tropical montane cloud forest, Soil Biology and Biochemistry, 41, 1338-1340, 2009a.

Zimmermann, M., Meir, P., Bird, M. I., Malhi, Y., and Ccahuana, A. J. Q.: Climate dependence of heterotrophic soil respiration from a soil-translocation experiment along a 3000 m tropical forest altitudinal gradient, European Journal of Soil Science, 60, 895-906, 10.1111/j.1365-2389.2009.01175.x, 2009b.

Zimmermann, M., Leifeld, J., Conen, F., Bird, M. I., and Meir, P.: Can composition and physical protection of soil organic matter explain soil respiration temperature sensitivity?, Biogeochemistry, 107, 423-436, 10.1007/s10533-010-9562-y, 2012.

12. Tables and Figures

Table 1. Site characteristics.

Elevation Band m a.s.l.	Habitat	Latitude	Longitude	Mean Annual Temperature °C	Mean Annual Precipitation mm	Bulk density 0-10 cm g cm-3	pH	Soil C:N 0-10 cm	Soil C 0-10 cm %	Mineral Soil Particle Size						Landforms	Plots	Flux Chambers
										0-10 cm			10-30 cm					
										Clay	Silt	Sand	Clay	Silt	Sand		n	n
600-1200	Premontane forest	12°53'43''	71°23'04''	20.5	5318	0.38 ± 0.03 (n = 21)	3.4 ± 0.1	11.3 ± 0.2	7.9 ± 0.5	5.4 ± 0.3	68.8 ± 3.9	25.4 ± 15.9	8.9 ± 1.8	81.0 ± 1.7	10.3 ± 2.5	ridge, slope, flat	3	15
1200-2200	Lower montane forest	13°2'56''	71°32'13''	17.2	2631	0.19 ± 0.03 (n = 17)	3.4 ± 0.1	14.5 ± 0.2	25.2 ± 1.3	3.6 ± 0.4	67.3 ± 4.2	29.3 ± 4.5	7.2 ± 0.4	83.8 ± 0.8	9.0 ± 0.9	ridge, slope, flat	3	15
2200-3200	Upper montane forest	13°11'24''	71°35'13''	10.7	1706	0.41 ± 0.02 (n = 12)	3.9 ± 0.1	16.8 ± 0.4	16.3 ± 1.0	5.1 ± 0.9	57.1 ± 7.9	37.9 ± 8.7	4.4 ± 2.0	46.5 ± 16.2	49.1 ± 18.1	ridge, slope	3	15
3200-3700	Montane grassland	13°07'19''	71°36'54''	9.3	2200	0.36 ± 0.03 (n = 27)	4.1 ± 0.1	12.9 ± 0.4	16.0 ± 1.0	2.6 ± 0.2	54.4 ± 3.0	43.0 ± 3.2	n/a	n/a	n/a	ridge, slope, flat, basin	4	20

Table 2. Description of the water-filled pore space and NO_3^- addition treatments for the laboratory manipulation experiments.

Habitat	Experimental Treatment	Soil Depth	Soil Type	WFPS %	Inorganic N added ng N (g soil)$^{-1}$	^{15}N Tracer	Replicate *n*
WATER-FILLED PORE SPACE							
Premontane forest	90 % WFPS	0-10	mineral	90	200	$^{15}NH_4^{15}NO_3$	5
	90 % WFPS	0-10	mineral	90	200	$^{14}NH_4^{15}NO_3$	5
	70 % WFPS	0-10	mineral	70	200	$^{15}NH_4^{15}NO_3$	5
	70 % WFPS	0-10	mineral	70	200	$^{14}NH_4^{15}NO_3$	5
	50 % WFPS	0-10	mineral	50	200	$^{15}NH_4^{15}NO_3$	5
	50 % WFPS	0-10	mineral	50	200	$^{14}NH_4^{15}NO_3$	5
	30 % WFPS	0-10	mineral	30	200	$^{15}NH_4^{15}NO_3$	5
	30 % WFPS	0-10	mineral	30	200	$^{14}NH_4^{15}NO_3$	5
Lower montane forest	90 % WFPS	0-10	mineral	90	200	$^{15}NH_4^{15}NO_3$	5
	90 % WFPS	0-10	mineral	90	200	$^{14}NH_4^{15}NO_3$	5
	70 % WFPS	0-10	mineral	70	200	$^{15}NH_4^{15}NO_3$	5
	70 % WFPS	0-10	mineral	70	200	$^{14}NH_4^{15}NO_3$	5
	50 % WFPS	0-10	mineral	50	200	$^{15}NH_4^{15}NO_3$	5
	50 % WFPS	0-10	mineral	50	200	$^{14}NH_4^{15}NO_3$	5
	30 % WFPS	0-10	mineral	30	200	$^{15}NH_4^{15}NO_3$	5
	30 % WFPS	0-10	mineral	30	200	$^{14}NH_4^{15}NO_3$	5
Upper montane forest	90 % WFPS	10-20	mineral	90	20	$^{15}NH_4^{15}NO_3$	5
	90 % WFPS	10-20	mineral	90	20	$^{14}NH_4^{15}NO_3$	5
	70 % WFPS	10-20	mineral	70	20	$^{15}NH_4^{15}NO_3$	5
	70 % WFPS	10-20	mineral	70	20	$^{14}NH_4^{15}NO_3$	5
	50 % WFPS	10-20	mineral	50	20	$^{15}NH_4^{15}NO_3$	5
	50 % WFPS	10-20	mineral	50	20	$^{14}NH_4^{15}NO_3$	5
	30 % WFPS	10-20	mineral	30	20	$^{15}NH_4^{15}NO_3$	5
	30 % WFPS	10-20	mineral	30	20	$^{14}NH_4^{15}NO_3$	5
Montane grassland	90 % WFPS	0-10	mineral	90	20	$^{15}NH_4^{15}NO_3$	5
	90 % WFPS	0-10	mineral	90	20	$^{14}NH_4^{15}NO_3$	5
	70 % WFPS	0-10	mineral	70	20	$^{15}NH_4^{15}NO_3$	5
	70 % WFPS	0-10	mineral	70	20	$^{14}NH_4^{15}NO_3$	5
	50 % WFPS	0-10	mineral	50	20	$^{15}NH_4^{15}NO_3$	5
	50 % WFPS	0-10	mineral	50	20	$^{14}NH_4^{15}NO_3$	5
	30 % WFPS	0-10	mineral	30	20	$^{15}NH_4^{15}NO_3$	5
	30 % WFPS	0-10	mineral	30	20	$^{14}NH_4^{15}NO_3$	5
NITRATE ADDITION							
Premontane forest	control	0-10	mineral	80	n/a	n/a	5
	+50 % background NO_3^-	0-10	mineral	80	780 ± 60	$K^{15}NO_3$	5
	+100 % background NO_3^-	0-10	mineral	80	1570 ± 120	$K^{15}NO_3$	5
	+150 % background NO_3^-	0-10	mineral	80	2350 ± 170	$K^{15}NO_3$	5
Lower montane forest	control	0-10	mineral	80	n/a	n/a	5
	+50 % background NO_3^-	0-10	mineral	80	700 ± 60	$K^{15}NO_3$	5
	+100 % background NO_3^-	0-10	mineral	80	1400 ± 120	$K^{15}NO_3$	5
	+150 % background NO_3^-	0-10	mineral	80	2100 ± 180	$K^{15}NO_3$	5
Upper montane forest	control	0-10	organic	80	n/a	n/a	5
	+50 % background NO_3^-	0-10	organic	80	90 ± 20	$K^{15}NO_3$	5
	+100 % background NO_3^-	0-10	organic	80	180 ± 50	$K^{15}NO_3$	5
	+150 % background NO_3^-	0-10	organic	80	270 ± 70	$K^{15}NO_3$	5
	control	10-20	mineral	80	n/a	n/a	5
	+50 % background NO_3^-	10-20	mineral	80	90 ± 40	$K^{15}NO_3$	5
	+100 % background NO_3^-	10-20	mineral	80	190 ± 70	$K^{15}NO_3$	5
	+150 % background NO_3^-	10-20	mineral	80	280 ± 110	$K^{15}NO_3$	5
Montane grassland	control	0-10	mineral	80	n/a	n/a	5
	+50 % background NO_3^-	0-10	mineral	80	30 ± 10	$K^{15}NO_3$	5
	+100 % background NO_3^-	0-10	mineral	80	60 ± 20	$K^{15}NO_3$	5
	+150 % background NO_3^-	0-10	mineral	80	90 ± 40	$K^{15}NO_3$	5

Table 3. Seasonal patterns in net N_2O flux, net inorganic N flux, and environmental variables. Lower case letters indicate difference among seasons within habitats (*t*-Test on Box-Cox transformed data, $P < 0.05$). Values reported here are means and standard errors.

Habitat	N_2O mg N-N_2O m^{-2} d^{-1}		WFPS %		Soil Temperature °C		Air Temperature °C		Oxygen %		NO_3^- µg N-NO_3^- (g resin)$^{-1}$ d^{-1}		NH_4+ µg N-NH_4^+ (g resin)$^{-1}$ d^{-1}	
	Wet Season	Dry Season	Wet Season	Dry Season	Wet Season	Dry Season	Wet Season	Dry Season	Wet Season	Dry Season	Wet Season	Dry Season	Wet Season	Dry Season
Premontane	0.71 ± 0.25 a n = 130	0.79 ± 0.26 a n = 98	51.9 ± 1.6 a n = 135	51.2 ± 2.1 a n = 135	20.7 ± 0.1 a n = 143	20.2 ± 0.1 b n = 120	21.5 ± 0.3 n = 143	20.4 ± 0.5 n = 120	19.4 ± 0.2 a n = 52	19.6 ± 0.2 a n = 36	23.2 ± 3.6 a n = 89	22.1 ± 2.1 a n = 96	31.4 ± 13.0 n = 90	11.3 ± 1.8 n = 95
Lower montane	0.09 ± 0.08 a n = 212	1.02 ± 0.58 b n = 137	42.2 ± 1.0 a n = 271	34.0 ± 1.4 b n = 179	18.1 ± 0.1 a n = 254	17.3 ± 0.2 b n = 164	18.9 ± 0.3 n = 254	18.3 ± 0.2 n = 164	19.2 ± 0.2 a n = 146	19.2 ± 0.1 a n = 81	11.8 ± 1.9 a n = 123	7.8 ± 1.4 a n = 94	20.2 ± 5.4 n = 124	8.6 ± 0.9 n = 93
Upper montane	0.06 ± 0.09 a n = 207	0.01 ± 0.11 a n = 146	42.0 ± 1.3 a n = 264	24.3 ± 1.4 b n = 180	11.8 ± 0.1 a n = 255	10.9 ± 0.2 b n = 165	12.8 ± 0.2 n = 255	12.5 ± 0.3 n = 165	18.7 ± 0.2 a n = 165	18.5 ± 0.2 a n = 109	1.4 ± 0.2 a n = 128	0.6 ± 0.2 b n = 91	22.5 ± 6.3 n = 129	11.3 ± 1.4 n = 93
Montane grassland	-0.01 ± 0.11 a n = 238	0.19 ± 0.12 a n = 160	88.5 ± 0.3 a n = 303	88.3 ± 0.5 a n = 184	11.6 ± 0.1 a n = 282	9.0 ± 0.2 b n = 205	11.4 ± 0.3 n = 284	12.0 ± 0.5 n = 205	12.2 ± 0.9 a n = 176	15.4 ± 0.8 b n = 117	1.5 ± 0.4 a n = 128	2.1 ± 0.4 a n = 81	17.8 ± 4.3 n = 135	7.2 ± 0.8 n = 84

1172 **Table 4.** Area- and seasonally-weighted annual estimates of N_2O, N_2, and total gaseous N

1173 flux

Elevation Band (m.a.s.l.)	Habitat	Surface Area (ha)	Fraction of Land Area	Fraction of Year Wet Season	Fraction of Year Dry Season	Nitrous Oxide Yield	Unweighted Nitrous Oxide Flux Wet Season kg N_2O-N ha^{-1} yr^{-1}	Unweighted Nitrous Oxide Flux Dry Season kg N_2O-N ha^{-1} yr^{-1}	Area-weighted Nitrous Oxide Flux Wet Season kg N_2O-N ha^{-1} yr^{-1}	Area-weighted Nitrous Oxide Flux Dry Season kg N_2O-N ha^{-1} yr^{-1}	Area-weighted and Seasonally-weighted Annual Estimate of N_2O Flux kg N_2O-N ha^{-1} yr^{-1}	Area-weighted and Seasonally-weighted Annual Estimate of N_2 Flux kg N_2-N ha^{-1} yr^{-1}	Area-weighted and Seasonally-weighted Annual Estimate of Total Gaseous N Flux kg N ha^{-1} yr^{-1}
600-1200	Premontane forest	733000	0.24	0.58	0.42	0.4 ± 0.05	2.59 ± 0.91	2.88 ± 0.95	0.63 ± 0.22	0.70 ± 0.23	0.66 ± 0.16	1.00 ± 0.29	1.66 ± 0.33
1200-2200	Lower montane forest	892000	0.30	0.58	0.42	0.19 ± 0.04	0.33 ± 0.29	3.72 ± 2.12	0.10 ± 0.09	1.10 ± 0.63	0.52 ± 0.27	2.21 ± 1.24	2.73 ± 1.26
2200-3200	Upper montane forest	807000	0.27	0.58	0.42	0.42 ± 0.05	0.22 ± 0.33	0.04 ± 0.40	0.06 ± 0.09	0.01 ± 0.11	0.04 ± 0.07	0.05 ± 0.09	0.09 ± 0.12
3200-3700	Montane grasslands	586000	0.19	0.58	0.42	0.61 ± 0.06	-0.04 ± 0.40	0.69 ± 0.44	-0.01 ± 0.08	0.13 ± 0.09	0.05 ± 0.06	0.03 ± 0.04	0.09 ± 0.07
Totals		3020000									**1.27 ± 0.33**	**3.29 ± 1.27**	**4.57 ± 1.31**

1174

Figure 1. Map of study sites across the Kosñipata Valley, Manu National Park, Peru.

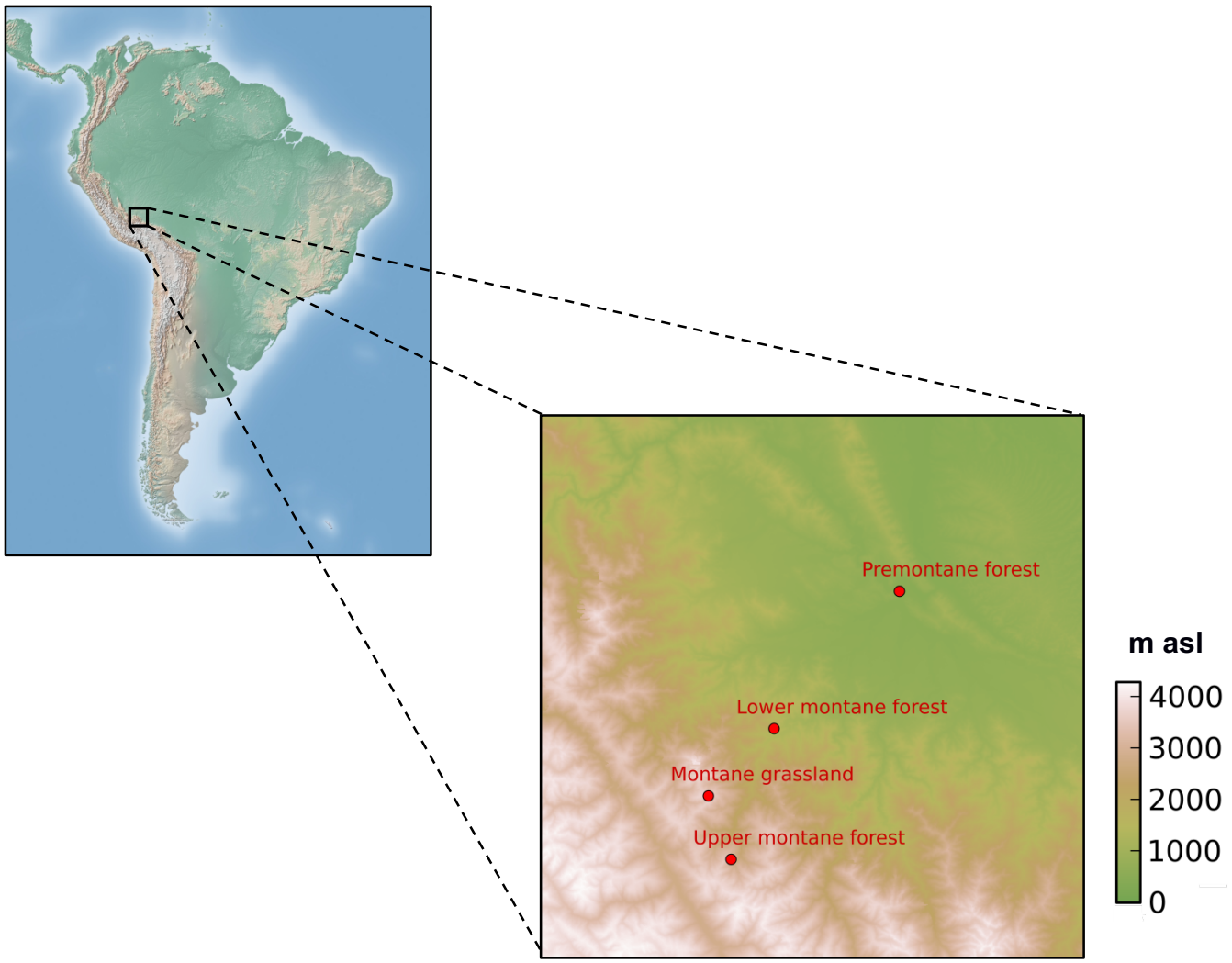

Figure 2. Plot-averaged (a) net N_2O flux, (b) water-filled pore space, and (c) resin-extractable NO_3^- flux among habitats. Boxes enclose the interquartile range, whiskers indicate the 90th and 10th percentiles. Lower case letters indicate statistically significant differences among means (Fisher's LSD, $P < 0.05$).

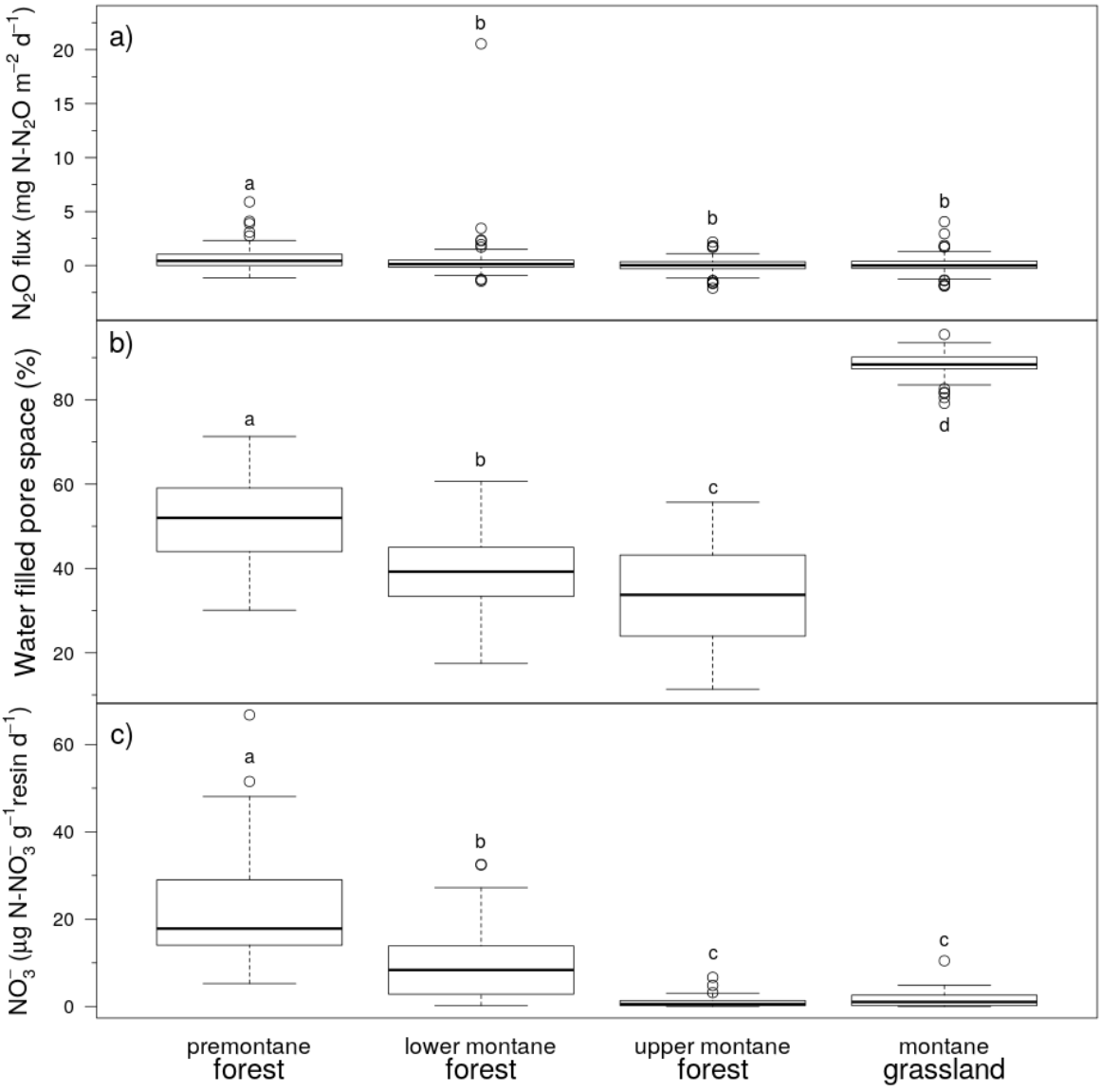

Figure 3. Time series of net N_2O flux and water-filled pore space (WFPS). Panels indicate data for (a) premontane forest, (b) lower montane forest, (c) upper montane forest, and (d) montane grasslands for the 30-month study period beginning in January 2011 and ending in June 2013. The broken horizontal line running across each panel denotes the overall mean N_2O flux or WFPS for that habitat. The broken line in each box indicate median values and the black lines indicate means. Dry and wet seasons are denoted by vertical shading on the graph, with the dry season (May to September) highlighted in white and the wet season (October to April) in light blue.

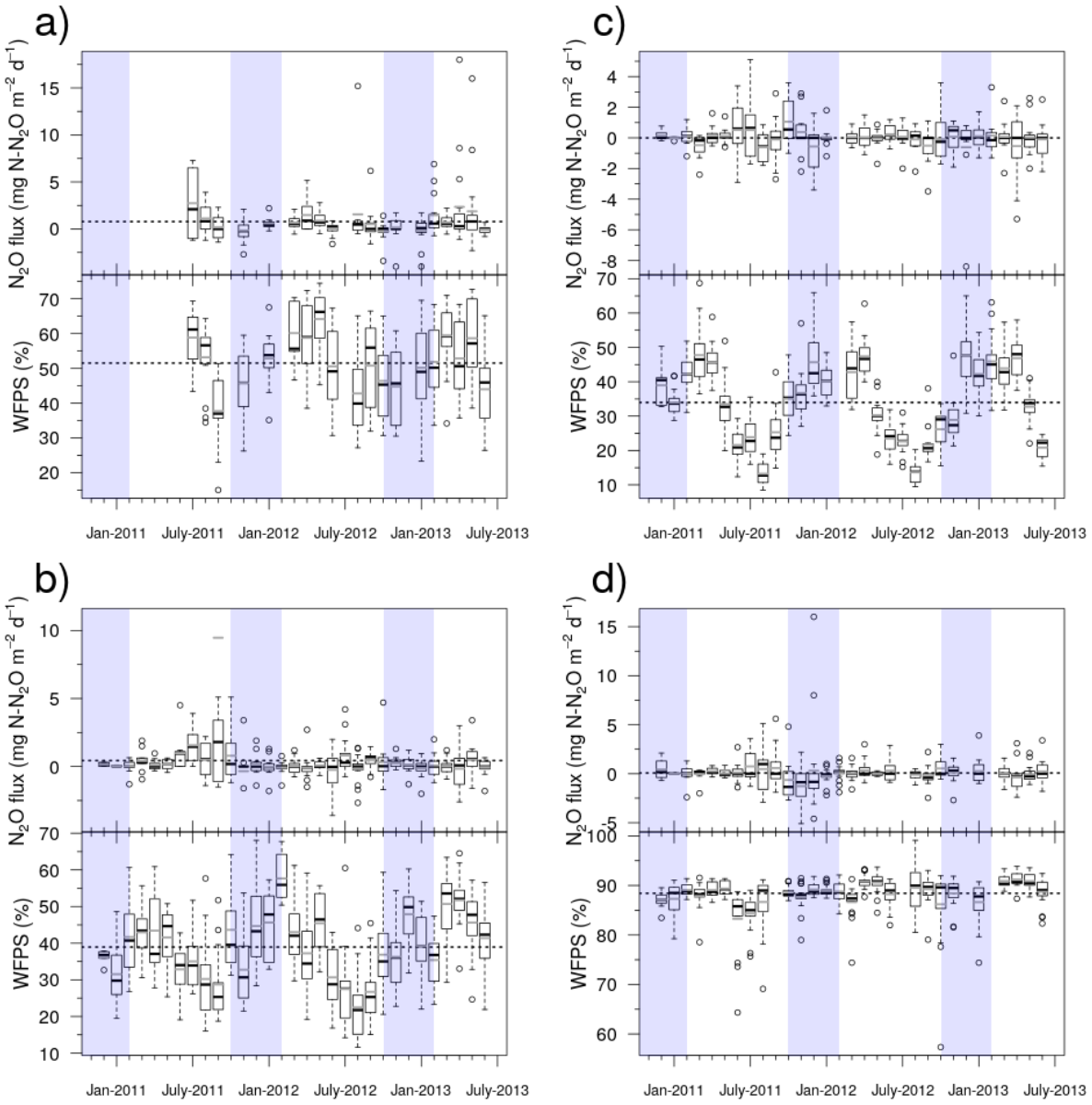

Figure 4. Total (a) ^{15}N-N_2O flux and (b) ^{15}N-N_2 flux during the early (≤24 hours) and late (>24 hours) incubation phases of the water-filled pore space (WFPS) experiment. Results from the 90 % WFPS treatment are shown in dark-grey, while data from the 70 %, 50 %, and 30 % WFPS treatments are shown in mid-grey, light-grey, and white, respectively. The bar charts show means and standard errors.

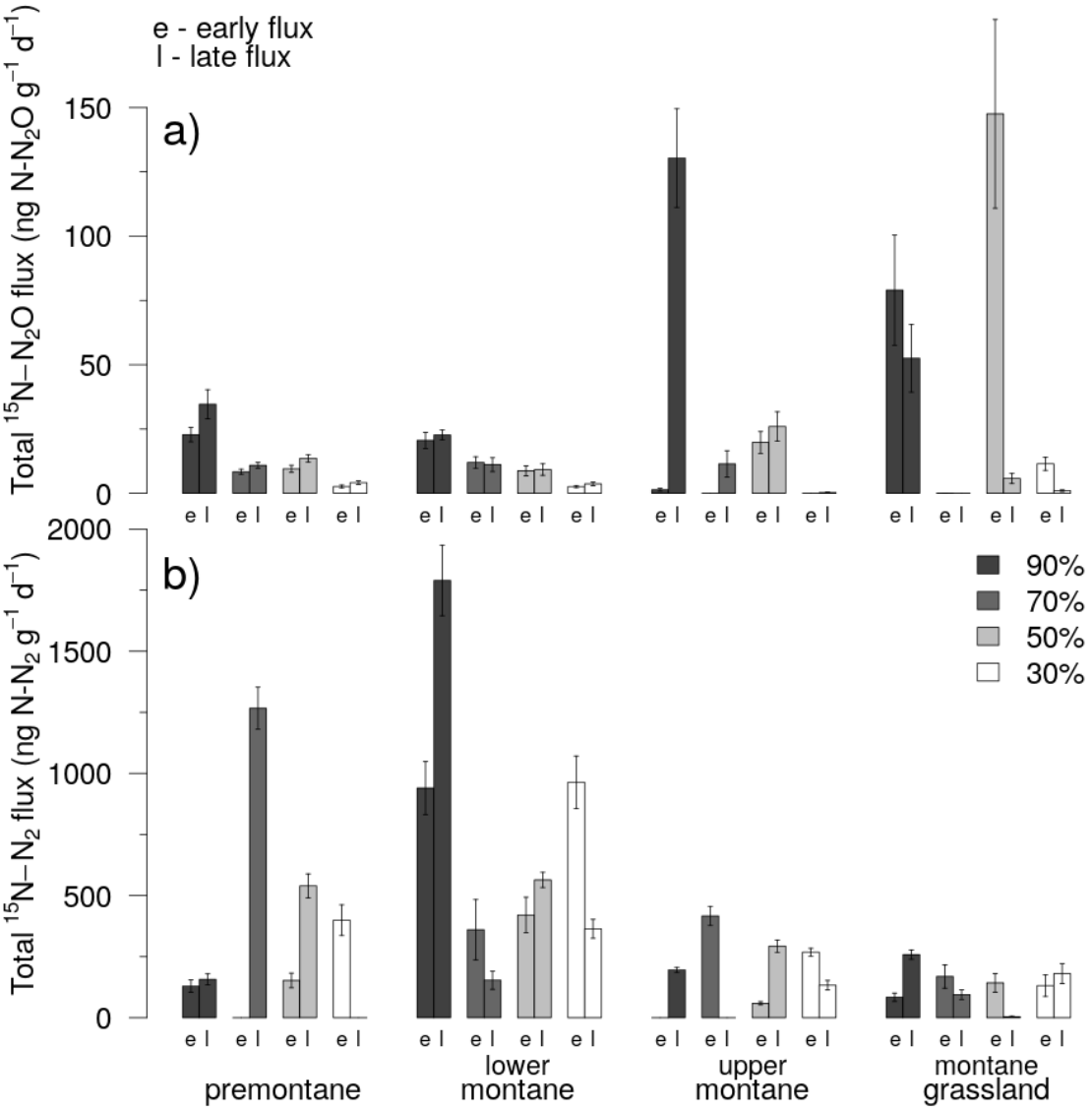

1221 **Figure 5.** (a) ^{15}N-N_2O flux and (b) ^{15}N-N_2 flux during the early (≤24 hours) and late (>24 hours)
1222 incubation phases of the NO_3^- addition experiment. Results from the +50 % NO_3^- addition are
1223 shown in dark-grey, while data from the +100 % and +150 % treatments are shown in mid-
1224 grey and light-grey, respectively. The bar charts show means and standard errors.

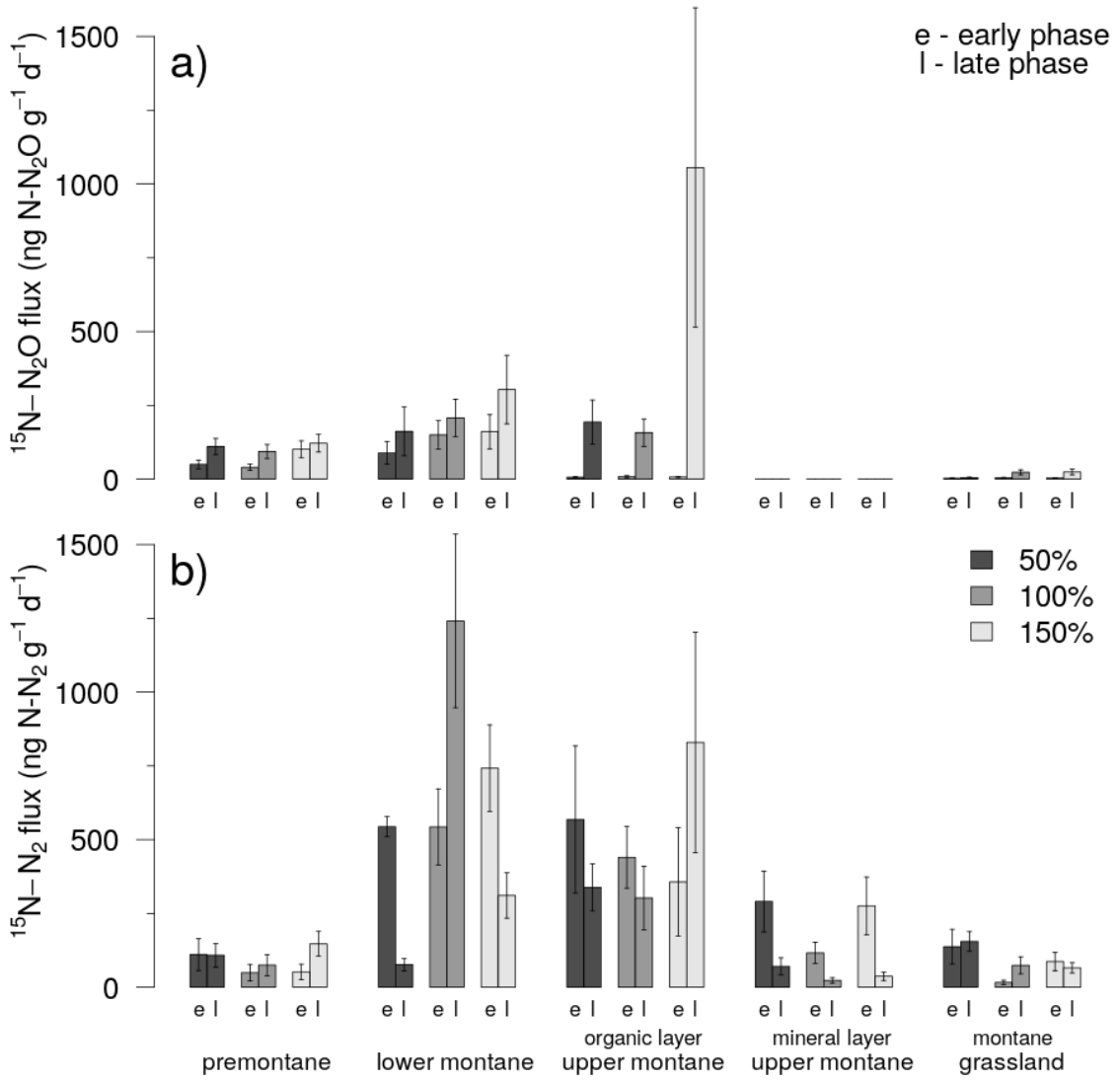

1225